THE CONTROL OF SWELLING AND SYNERESIS

IN BOROSILICATE GELS USING

COLLOIDAL PHENOMENA

by

BARBARA LINDHOLM ANGELL

B.S., Kansas State University, 1983

A MASTER'S THESIS

submitted in partial fulfillment of the
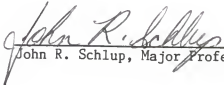
requirements for the degree

MASTER OF SCIENCE

College of Engineering
Department of Chemical Engineering

KANSAS STATE UNIVERSITY
Manhattan, Kansas

1986

Approved by:

John R. Schlup, Major Professor

Acknowledgments

I would like to thank Professor John Schlup for his guidance throughout my graduate studies and his concern for both my professional and personal well being. Larry Glasgow and John Matthews have also helped me to complete this research.

Gratitude is due to the National Science Foundation for supporting this research through grant number CPE-8404348. In addition, my graduate studies at Kansas State University were financially assisted by a fellowship from Dow Chemical.

A special thanks is owed my parents, John and Mildred Lindholm, for their encouragement throughout my academic endeavors. Finally, I am indebted to my husband, Randall, for his unending support. Without his help, this thesis would not have been possible.

<div align="right">Barbara L. Angell</div>

Table of Contents

List of Figures

List of Tables

I. <u>Introduction</u>

Background

Sol-gel techniques have been used to prepare materials ranging from thin films of glass to monolithic ceramic bodies. Although many procedures are available from the literature for preparing these materials, the factors which control the properties of the final product are only partially understood. In particular, the colloidal phenomena associated with sol-gel systems have not been systematically investigated.

Before this discussion continues, several terms should be defined. A colloidal system involves a mixture of two substances; a dispersed phase (or colloid) is uniformly distributed in a dispersion medium. Colloids are small particles with at least one dimension on the order of a few micrometers. Sols are liquid colloidal dispersions in which settling of the colloidal particles does not occur on a practical time scale. Gels occur when the dispersed phase combines with the continuous phase to produce a network. The mechanical properties of a gel are similar to those of a solid. Syneresis is the opposite of swelling and involves the spontaneous exudation of the liquid component from the gel.

Sol-gel methods involve these three main parts: gel synthesis, post-gelation and sintering (see Figure 1.1) [1]. The gel synthesis can proceed by two different routes to produce either colloidal or polymeric gels. The colloidal path starts with the preparation of the sol. As the solvent evaporates, the dispersed and continuous phases combine to form a network and a gel is created. The polymeric process involves a solution of inorganic monomers. When two polymer species randomly collide, dehydration and hydrolysis reactions join the two species, resulting in one longer polymer. As this polycondensation continues, the polymers crosslink to

form networks.

In the post-gelation step, the gel is rinsed to remove the volatiles. There is a small volume change associated with the rinsing, but this is not the intent of this step. Rather, the purpose is to wash away unreacted monomers and initiators as well as the solvent and reaction by-products. The rinsed gel is then dried to remove the water. Lengthy drying times are required to minimize the internal stresses caused by the volume changes on drying and the capillary forces in the gel pores. When drying begins, the gel network is flexible and can rearrange as the water evaporates. Later, as the gel network becomes more restricted and the pores are only partially filled with water, liquid-air interfaces develop. These interfaces cause capillary stresses which result in mud cracking. The final step in the sol-gel method for preparing dense ceramics is sintering.

Because the final products have better homogeneity and purity, sol-gel methods are suitable for making specialty ceramics. However, with the high cost of the raw materials, it is improbable that these techniques can be competitive for conventional glass products such as flat glass, containers and common fibers. A list of advantages and disadvantages of sol-gel methods is presented in Table 1.1. Sol-gel methods are feasible when the advantages gained from the technique are necessary and the resulting product can be priced to make a profit.

Problem

The major disadvantage of sol-gel methods is the large uncontrolled shrinkage of the gel during the drying and sintering processes [2]. With previous studies, when the final product developed cracks the gel reactions were changed by varying the reactant concentrations, solvents or other parameters. Few attempts were made to change the gel once formed.

The research presented in this thesis is an initial attempt to separate the effects due to the gel synthesis from effects due to swelling or syneresis in the post-gelation step (Figure 1.2). The goal was to reduce the problems associated with the drying process by first minimizing the gel volumes in the wet state. This was accomplished by placing the gels in solutions which might induce syneresis. An investigation of the colloidal behavior of gels in various solutions would reveal the effectiveness of such a procedure.

The experiments were conducted on borosilicate gels since several synthesis procedures were available in the literature. However, no post-gelation studies involving borosilicate gels had been published. The gel synthesis procedure used was repeated as precisely as possible in order to minimize the differences in the gels due to synthesis parameters. Therefore, any changes in the gel volumes following the rinsing and swelling or syneresis processes were attributed to these operations.

Approach

Many different solvent and gel preparation parameters possibly could bring about the volume changes desired. Some initial screening was necessary to keep the experimentation on a manageable level. The results of similar investigations of other systems provided a starting point. Tanaka examined the effects of many variables on hydrolyzed polyacrylamide gel phase transitions [3,4,5]. By studying the variables independently, Tanaka found that increasing the temperature, the acetone concentration, the pH or the salt concentration of the soaking solution caused the gel to collapse. This work was proposed to determine if similar behavior could be demonstrated with inorganic gels. A 2^4 factorial experiment was conducted to identify important variables and their effects on the solvent content

of SiO_2 and $SiO_2 \cdot B_2O_3$ gels. The solvent variables investigated were electrolyte valence, electrolyte concentration and pH, while the gel preparation variables were composition and rinsed state. Graphical and computational analysis determined how these variables influenced the water-to-solids mass ratio of the wet gels.

Once the significant variables were identified, the colloidal behavior associated with continuous changes in these variables was investigated. A more detailed, mechanistic experiment was planned to provide this information. This experiment included five different gel compositions and eleven solutions with varying electrolyte concentrations. The other variables were held constant at the levels at which the more dense gels were produced. Both water-to-solids mass ratios and specific volume measurements were conducted to evaluate the volume changes.

The surface area could be an important parameter. A significant decrease in surface area would not only indicate a reduction in the gel volume, but would also show that the number and/or sizes of the pores had diminished. Both conditions aid in minimizing the mud cracking problems which occur upon drying. Therefore, it would be beneficial to be able to measure the surface area of the gel.

Various surface area measurement techniques were considered before an appropriate method was chosen. Dry surface area measurements, such as the BET technique based upon gas adsorption, would not accurately reflect the pore conditions in the wet state since the gels usually collapse when dried [6]. Dye adsorption involves a liquid-solid system; however, there is uncertainty about the size, configuration and orientation of the adsorbing dye molecule [7]. Negative adsorption can be used to determine the specific surface areas of suspended charged particles without knowledge

of the adsorbing molecule or ion's size. In addition, the measurements are made in solutions such as the aqueous NaCl mixtures used elsewhere in this investigation. When placed in an electrolyte solution, a charged surface, such as a borosilicate gel, will attract counterions and repel co-ions. Negative adsorption techniques relate the increase in co-ions in the bulk solution to the area of the charged surface. Although negative adsorption has been used to determine the surface areas of clays and other materials, a negative adsorption procedure is not available in the literature. Thus, a technique was developed which provided suitable surface area measurements of the wet borosilicate gels.

References

[1] Zelinski, B. J. J. and D. R. Uhlmann. "Gel Technology in Ceramics,"
     Journal of Physical Chemistry and Solids, 45: 1069-1090 (1984).

[2] Mackenzie, J. D. "Applications of Sol-Gel Methods for Glass and
     Ceramics Processing" in _Ultrastructure Processing of Ceramics, Glass
     and Composites_, edited by Larry L. Hench and Donald R. Ulrich, New
     York: John Wiley and Sons, 1984.

[3] Tanaka, Toyoichi. "Gels," _Scientific American_, _244_: 124-138 (1981).

[4] Tanaka, Toyoichi. "Collapse of Gels and the Critical Endpoint,"
     Physical Review Letters, _40_: 820-823 (1978).

[5] Tanaka, Toyoichi, _et al_. "Phase Transitions in Ionic Gels," _Physical
     Review Letters_, _45_: 1636-1639 (1980).

[6] Adamson, Arthur W. _Physical Chemistry of Surface_, _4th Edition_.
     New York: John Wiley and Sons, 1982.

[7] James, Robert O. and George A. Parks. "Characterization of Aqueous
     Colloids by Their Electrical Double-Layer and Intrinsic Surface
     Chemical Properties" in _Surface and Colloid Science, Volume 12_,
     edited by Egon Matijevic. New York: John Wiley and Sons, 1980.

Table 1.1. Advantages and Disadvantages of the Sol-Gel
Method over Conventional Melting for Glass.

<div align="center">Advantages</div>

1. Better homogeneity—from raw materials.

2. Better purity—from raw materials.

3. Lower temperature of preparation:

    (a) save energy;
    (b) minimize evaporation losses;
    (c) minimize air pollution;
    (d) no reactions with containers, thus purity;
    (e) bypass phase separation;
    (f) bypass crystallation.

4. New noncrystalline solids outside the range of
    normal glass formation.

5. New crystalline phases from new noncrystalline
    solids.

6. Better glass products from special properties
    of gel.

7. Special products such as films.

<div align="center">Disadvantages</div>

1. High cost of raw materials.

2. Large shrinkage during processing.

3. Residual fine pores.

4. Residual hydroxyl.

5. Residual carbon.

6. Health hazards of organic solutions.

7. Long processing times.

Source: J. D. Mackenzie, _Journal of Non-Crystalline
Solids_, 48: 1 (1981).
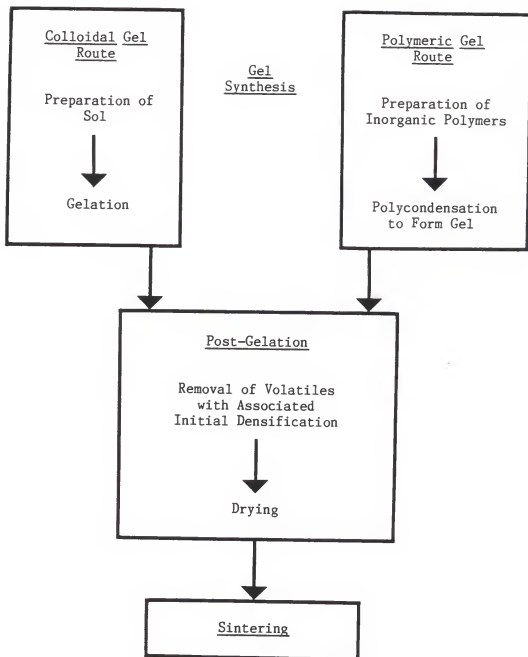
Figure 1.1. Main Steps in Sol-Gel Methods.
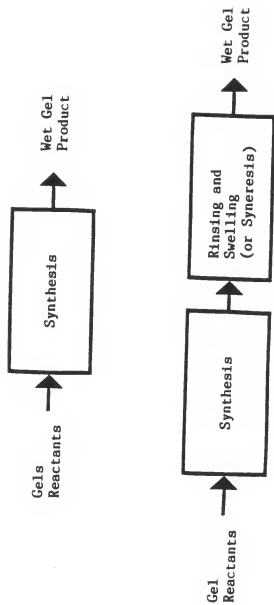
Figure 1.2. Schematic Diagram Comparing the Approach of Previous Studies to the Approach Used in This Research.

II. The Factorial Design Experiment

Background

Experimental programs often evolve through several stages. As a program progresses, the number of independent variables decrease while the model's complexity and accuracy increase [1]. First, all relevant independent variables are screened using tests designed to identify the important parameters and their approximate effect on the response value studied. Screening experiments typically deal with six to thirty continuous and/or discrete candidate variables. The variables found to be trivial are held constant at suitable levels during subsequent experimentation. Next, a limited response surface experiment typically looks at the three to eight variables found to be significant. Here an experiment is planned to estimate linear effects and interactions of the variables over the experimental region. After this, a response surface experiment will give more accurate predictions of behavior over the range of interest for two to six continuous variables. A mechanistic experiment will produce a more sophisticated estimate of the effects of one to five variables. Such a model can be applied to conditions outside the experimental region. The final stage of testing is sampling experiments which characterize the changes of the final product under standard operating conditions.

The most appropriate stage at which to begin a particular investigation depends on what is known about the system to be studied. If little is known about the subject, a screening experiment may be necessary. However, when extensive information about similar systems is available, a limited response surface experiment would be a more productive initial experiment.

The purpose of this study was to investigate the volume changes of

borosilicate gels in various soaking solutions. The initial understanding of such changes comes from knowledge of the system (e.g. osmotic pressure [2]). Previous investigations have focused on organic gels. For example, Tanaka [3] examined the effects of many variables on hydrolyzed polyacryl-amide gel phase transitions. By studying the variables independently as in mechanistic experiments, Tanaka found that increasing the temperature, the acetone concentration, the pH or the salt concentration of the soaking solution caused the gel to collapse. This work was proposed to examine similar effects on inorganic gels with a limited response. The variables of the soaking solution considered were electrolyte valence, salt concentration and pH. Tests were conducted on both SiO_2 and $SiO_2 \cdot B_2O_3$ gels in rinsed and unrinsed states. The volume changes were expressed as a water-to-solids mass ratio. A two-level full factorial designed experiment with a center point was used for studying the linear effect and interactions of these variables.

Factorial Experiment

Factorial experiments are a series of trials with the independent variables chosen to maximize the information obtained [4]. This informa-tion makes it possible to determine how each individual variable and all combinations of the variables change the properties studied. Thus, one is able to eliminate the variables found to have little effect over the range of the experiment and discover how to best manipulate important variables in further processes. Statistical principles are used to insure that a sufficient number of trials are planned to identify results caused by programmed changes in variables and not by experimental noise. Bias errors, such as the differences in the gels from batch to batch, are minimized by conducting the trials in a random order.

The number of experimental runs, or design points, n, required for a factorial design is calculated as follows:

$$n = \ell^p \qquad (2.1)$$

where

p = number of factors or variables

ℓ = levels per factor

The variables considered in this factorial experiment were tested at a high and a low level. There should be enough range between the high and low levels that the difference is clearly larger than the experimental error. A bold approach is necessary since the model developed is only valid in the range tested. Since there were four factors (valence, concentration, pH and full rinse/no rinse) and each was considered at two levels, sixteen experiments were conducted under different conditions. This 2^4 factorial design experiment was used on each of two borosilicate gel compositions, SiO_2 and $SiO_2 \cdot B_2O_3$.

The two level experimental model is developed for linear behavior between design points. Since this may not be accurate, it is best to provide an estimate of the overall curvature by running an experiment using the average value of each continuous variable. Center point response values are compared to the linear model prediction, that is, the average of the design point response values. If these numbers differ significantly based upon established statistical procedures, the curvature is significant and should be considered in further testing and model designs. Thus, an additional set of experimental conditions was developed to study curvature bringing the total number of trials to seventeen.

Standard two-level factorial design patterns are written with codes.

The high level variable condition is commonly coded as "+," while the low level variable condition becomes "-." The average of these values, the center point, is labeled as "0." The 2^4 factorial design pattern with a center point is shown in Table 2.1. Replicate experiments were conducted to increase the precision of the study. Any bias error was reduced by running the trials in a random order.

A 2^4 factorial is geometrically represented as two three-dimensional cubes (Figure 2.1a). Each dimension of the figure depicts a variable. The parameters of the soaking solution, valence, concentration and pH, are illustrated by the x_1, x_2 and x_3 axes, respectively. The origin of each axis is the low level of the variable and the axis extends to the high level of the variable. The left cube also includes the low level of the fourth parameter, no rinsing, while the right cube includes the high level, full rinsing. Thus, all sixteen corners of the cubes represent a different set of experimental conditions.

The main effect of a variable x_1 is calculated using the response values on the two planes at the high and low ends of its axis in each cube (Figure 2.1b). This main effect is valid over all ranges of the other variables, since all combinations of these variables are represented. This same pattern of high and low range planes is repeated as the data for the sixteen design points is rearranged to calculate the main effect of all four variables. Since it uses all the design points in every calculation, the factorial experiment has hidden replication which eliminates experiments without sacrificing confidence. Different mathematical combinations of these same sixteen design points yield information about interactions between two or more variables. For example, the effect of x_1 may vary at different levels of x_2 and x_3. Such interactions become more obvious with

a comparison of diagonally opposite pairs of points. On the 2^4 factorial geometrical representation, this effect involves the four corners of diagonal planes (Figures 2.1c and 2.1d).

<u>Experimental</u> <u>Procedure</u>

This experiment was conducted using the variables and ranges listed in Table 2.2. The individual trial conditions were determined from the 2^4 factorial design pattern presented earlier (Table 2.1). These trials were duplicated and randomized to produce the actual order in which the experiments were conducted (Table 2.3). This plan was used for both the SiO_2 and the $SiO_2 \cdot B_2O_3$ gels.

The experimental procedure has been divided into the following three parts.

    (1) borosilicate gel production

    (2) design variable changes

    (3) response evaluation

<u>Borosilicate</u> <u>Gel</u> <u>Production</u>. The experimental procedure used for making borosilicate gels was originally derived from three published procedures [5,6,7] and modified during initial testing. The following procedure was used to make SiO_2 and $SiO_2 \cdot B_2O_3$ gels for the factorial experiment.

Apparatus:

    (1) 500 ml polypropylene beaker

    (2) aluminum foil, about 4 inches square with a hole cut in the center

    (3) electric stirrer, variable speed

    (4) stirring blade, stainless steel

    (5) water bath, constant-temperature to within 0.5°C

(6) thermometer

(7) ring stand and clamps to support the electric stirrer and hold the beaker

(8) graduated cylinders, one for each chemical used

(9) 50 ml polypropylene beakers, one for each 8 ml of liquid gel produced

(10) Parafilm, used to seal tops of 50 ml beakers

(11) spatula, metal

Materials:

(1) tetraethyl orthosilicate, $Si(OC_2H_5)_4$

(2) trimethyl borate, $B(OCH_3)_3$, 99%

(3) ethanol, C_2H_5OH, 100%

(4) mildly acidic water mixture, (0.15 mol HCl/1 liter H_2O) made with hydrochloric acid, HCl, and deionized water, H_2O

Preparation of equipment:

(1) Fill the constant temperature bath with tap water and maintain this at 50 °C throughout the run.

(2) Partially immerse the 500 ml beaker in the water, stabilize with the clamps and ring stand.

(3) Mount the stirrer to the ring stand and position it so that the blade is in the 500 ml beaker.

Procedure:

(1) Pour 45 ± 0.5 ml of $Si(OC_2H_5)_4$ into the beaker.

(2) Start stirrer at about 2 revolutions per second.

(3) Hydrolyze the $Si(OC_2H_5)_4$ by adding a mixed solution of 10 ± 0.1 ml of C_2H_5OH and 5 ± 0.1 ml of HCl/H_2O solution.

(4) Cover the top of the beaker with the aluminum foil so that the stirring blade enters through the center hole in the foil.

(5) Continue to stir this mixture at 50°C for 1 hour.

(6) If the final product is to be SiO_2, continue with step 8. If the final product is to be $SiO_2 \cdot B_2O_3$, add 45 ± 0.5 ml of $B(OCH_3)_3$ to the hydrolyzed solution.

(7) Continue to stir this mixture at 50°C for 2 hours.

(8) Add 5 ± 0.1 ml HCl/H_2O solution.

(9) Continue to stir this mixture at 50°C for 1 hour.

(10) Remove the 500 ml beaker and its contents.

(11) Pour 8 ml portions of the liquid gel mixture into the 50 ml polypropylene beakers.

(12) Seal the beakers with Parafilm.

(13) Set aside a few days for gelation.

(14) When the gels are viscous enough that they do not change shape when the 50 ml beakers are turned upside down, remove the gels with the metal spatula.

$\underline{Designed}$ $\underline{Variable}$ $\underline{Changes}$. It was assumed that all SiO_2 and $SiO_2 \cdot B_2O_3$ gels were identical. Randomization minimized the bias error due to actual differences in the gels. Further treatment of individual gels were conducted according to the 2^4 factorial experiment design (Table 3).

Individual gels that were to be fully rinsed were placed in 100 ml of deionized water and allowed to soak for one hour. The water was drained and replaced with fresh deionized water every hour for a total of five hours soaking time. The center point half rinses were conducted in much the same way, except that the one hour soaking times were halved to 30 minutes. The gels that were not to be rinsed were immediately placed

in their appropriate soaking solutions.

Seven solutions were made to accomodate all experimental conditions. These included 1.0 N Al^{3+} at 4 pH and at 10 pH, 1.0 N Na^+ at 4 pH and at 10 pH, 0.0 N at 4 pH and at 10 pH, and 0.5 N Mg^{2+} at 7 pH. The lower concentration level for both Al^{3+} and Na^+ was supplied by the same two 0.0 N solutions.

The gels were placed in 300 ml polypropylene beakers with 100 ml of the electrolyte solution desired. The beakers were sealed with Parafilm and set aside. After a two week soaking period, one third of the gel sample was removed for drying. A second piece of the gel was taken out of the solution a week to ten days later. The last section was removed in another week to ten days. The soaking times were varied to determine when equilibrium was reached.

Response Evaluation. The change in gel volume was measured as a water-to-solids mass ratio. An increase in the solvent content of a gel would indicate an increase in gel volume. Similarly a decrease in solvent content would mean a decrease in volume. This was determined by a loss on dehydration technique which involved thoroughly drying the gel in an oven (LOD/110°C). When the gels were removed from the soaking solutions, they were blotted on a paper towel to remove surface moisture. The wet gels were then weighed and placed into an oven set at 110°C. The gels were dried to constant weights over a period of two to four days. The mass of the liquid was the mass lost through evaporation, while the mass of the solids was the mass of the dried gel. The various soaking times showed no trend in the individual run results, so all samples were assumed to be at equilibrium within two weeks. The results from each run were averaged and these values were averaged for each trial.

Graphical and Computational Analysis

Trends in the results can be seen in graphical plots similar to Figure 2.1a. The computational analysis is performed with the use of a table designed for a 2^4 factorial experiment (Table 2.4 [1]). The trial average responses are listed in the second column. In column three, the mean of these values is calculated. In subsequent columns, all trial response values with a "+" sign in the column are added together and this total is written in the "sum +" row. Likewise, the sum of the trial response values with a "−" sign is recorded in the "sum −" row. As a mathematical check, the "sum +" and the "sum −" values are combined to get the overall sum which should be the same for all columns. The difference is calculated by subtracting the "sum −" from the "sum +" and the effect is this difference divided by the number of positive signs in that column. This final value represents the main effect for the single variable at the top of that column or the interaction effect for the two or more variables in that column.

The curvature is calculated as the average of the center points minus the mean determined in the third column. This curvature effect is recorded at the bottom of Table 2.4.

The computed factor effects are compared to the minimum significant factor effect calculated using the following equation:

$$[\min] = ts\sqrt{2/mk} \tag{2.2}$$

where

t = the value of Student's "t" at the desired probability level
   for the number of degrees of freedom in the estimate "s"
s = pooled standard deviation of a single response observation
m = the number of + signs in the column

k = the number of replicates of each trial

Similarly, the curvature effect is compared to the minimum significant curvature:

$$[\min C] = ts\sqrt{1/mk + 1/c} \tag{2.3}$$

where

c = the number of center point values

These values are also listed in Table 2.4. If any factor effects or interaction effects are larger in magnitude than the minimum significant factor effect, then the variable or variables associated with them are determined to be important to the response value changes. Likewise, a curvature effect greater than the minimum significant curvature shows that at least one variable has nonzero curvature associated with it.

Experimental Results

The seventeen averaged trial values found for SiO_2 and $SiO_2 \cdot B_2O_3$ are presented in Figures 2.2 and 2.3. Graphical comparison of the valence (x_1) planes showed that the mass liquid/mass solid response values tended to increase with increasing valence; however, there was an exception for the condition of low normality, high pH and full rinsing for both SiO_2 and $SiO_2 \cdot B_2O_3$. A similar scrutiny of the other planes revealed that the response values usually decreased with increasing normality (x_2) and increased with rinsing (x_4). The SiO_2 gel response values generally increase with increasing pH (x_3), while the $SiO_2 \cdot B_2O_3$ gels showed the opposite effects. A comparison of the SiO_2 and $SiO_2 \cdot B_2O_3$ results indicated that the values were consistently higher for $SiO_2 \cdot B_2O_3$ gels.

The computational analysis was conducted in Tables 2.5 and 2.6. The minimum significant factor effect and minimum significant curvature

calculations are in Appendix A. The effects found to be meaningful were marked with an asterisk in Tables 2.5 and 2.6. Valence, concentration and the interaction of these variables were important for SiO_2 at a 90% probability level. The rinsing variable, the interactions between concentration and rinsing, and these two variables plus pH were also significant. Rinsing was the only variable with a significantly high factor effect for $SiO_2 \cdot B_2O_3$ at a 90% probability level. At a somewhat lower probability level, the factor effects of the other three variables as well as valence and concentration combination and the pH and rinsing combination were large. All the other effects including curvature were too small to be significant.

The graphical and computational analyses were repeated using an adjusted response value. Unrinsed and unsoaked "blank" gels were dried in the same manner as the experimental samples. A normalized difference was calculated using the average of these blank values and each experimental response value as follows:

$$\text{adjusted value} = \frac{\text{blank value} - \text{experimental value}}{\text{blank value}} \quad (2.4)$$

These adjusted values and their graphical and computational analyses are presented in Appendix B. The results identified the same significant factor effects and confirmed the previous analyses.

Modeling the System

The factor effects calculated in Tables 2.5 and 2.6 represent the difference between the high and low level response values. Thus, half of the factor effect is the change in the response associated with the change from center point conditions to the high or low level state of that variable or·combination of variables. The model for a two—level

factorial is written in terms of the coded factors x_j and half of the corresponding factor effects [1]:

$$\hat{y} = b_0 + b_1 x_1 + b_2 x_2 + b_3 x_3 + b_4 x_4 + b_{12} x_1 x_2 + b_{13} x_1 x_3 + b_{14} x_1 x_4$$
$$+ b_{23} x_2 x_3 + b_{24} x_2 x_4 + b_{34} x_3 x_4 + b_{123} x_1 x_2 x_3 + b_{124} x_1 x_2 x_4$$
$$+ b_{134} x_1 x_3 x_4 + b_{234} x_2 x_3 x_4 + b_{1234} x_1 x_2 x_3 x_4 \qquad (2.5)$$

where

$$\hat{y} = \text{predicted response}$$
$$x_j = \frac{\text{factor level} - (Hi + Lo)/2}{(Hi - Lo)/2}, \text{ jth factor}$$
$$\text{for factor level Hi, } x_j = 1$$
$$\text{for factor level Lo, } x_j = -1$$
$$b_j = 1/2(\text{factor effect for } x_j)$$
$$b_{jj'} = 1/2(\text{interaction effect for } x_j x_{j'})$$
$$b_{jj'j''} = 1/2(\text{interaction effect for } x_j x_{j'} x_{j''})$$
$$b_{jj'j''j'''} = 1/2(\text{interaction effect for } x_j x_{j'} x_{j''} x_{j'''})$$
$$b_0 = \bar{y}$$

The model for SiO_2 follows:

$$\hat{y} = 1.480 + 0.075x_1 - 0.075x_2 + 0.037x_3 + 0.058x_4 + 0.075x_1 x_2$$
$$- 0.0075x_1 x_3 - 0.010x_1 x_4 - 0.032x_2 x_3 + 0.058x_2 x_4 - 0.0255x_3 x_4$$
$$- 0.0175x_1 x_2 x_3 - 0.002x_1 x_2 x_4 - 0.0225x_1 x_3 x_4 + 0.055x_2 x_3 x_4$$
$$+ 0.036x_1 x_2 x_3 x_4 \qquad (2.6)$$

This model was simplified by eliminating the variables and interactions found to be insignificant in the computational analysis.

$$\hat{y} = 1.480 + 0.075x_1 - 0.075x_2 + 0.058x_4 + 0.075x_1 x_2 + 0.058x_2 x_4$$
$$+ 0.055x_2 x_3 x_4 \qquad (2.7)$$

The model for $SiO_2 \cdot B_2O_3$ follows:

$$\hat{y} = 2.797 + 0.1525x_1 - 0.171x_2 - 0.115x_3 + 0.3465x_4 + 0.136x_1x_2$$
$$+ 0.0775x_1x_3 + 0.004x_1x_4 + 0.0045x_2x_3 + 0.025x_2x_4 + 0.101x_3x_4$$
$$+ 0.076x_1x_2x_3 + 0.0405x_1x_2x_4 + 0.0135x_1x_3x_4 - 0.071x_2x_3x_4$$
$$+ 0.078x_1x_2x_3x_4 \tag{2.8}$$

If all variables found to be insignificant in the computational analysis are omitted, only the rinsing variable remains.

$$\hat{y} = 2.797 + 0.3465x_4 \tag{2.9}$$

However, several factor effects were sizable although they were less than the minimum significant factor effect at a 90% confidence limit. If these terms are included, the $SiO_2 \cdot B_2O_3$ model becomes

$$\hat{y} = 2.797 + 0.1525x_1 - 0.171x_2 - 0.115x_3 + 0.3465x_4 + 0.136x_1x_2$$
$$+ 0.101x_3x_4 \tag{2.10}$$

The x_j's can be calculated for any level within the limits of the experiment as follows:

$$x_1 = \frac{\text{valence} - (3 + 1)/2}{(3 - 1)/2} = \text{valence} - 2 \tag{2.11}$$

$$1 \leq \text{valence} \leq 2$$

$$x_2 = \frac{\text{concentration} - (1.0 + 0)/2}{(1.0 - 0)/2} = \frac{\text{concentration} - 1/2}{1/2} \tag{2.12}$$

$$0.0 \text{ N} \leq \text{concentration} \leq 1.0 \text{ N}$$

$$x_3 = \frac{\text{pH} - (10 + 4)/2}{(10 - 4)/2} = \frac{\text{pH} - 7}{3} \tag{2.13}$$

$$4 \leq \text{pH} \leq 10$$

$$x_4 = \frac{\text{total rinsing time} - (5 \text{ hr} - 0 \text{ hr})/2}{(5 \text{ hr} - 0 \text{ hr})/2}$$

$$= \frac{\text{total rinsing time} - 2\ 1/2}{2\ 1/2} \tag{2.14}$$

$0 \text{ hr} \leq \text{rinsing time} \leq 5 \text{ hr}$

(total rinsing time based on 5 rinses of equal length)

The normalized differences between the actual and predicted responses for each of the sixteen experimental conditions are presented in Tables 2.7 and 2.8. The predicted values for equations 2.6 and 2.8 were within 0.1% of the actual values for the design points. The simplified models (equations 2.7 and 2.10) were not as accurate; however, over 90% of their predictions were within 10% of the actual response value. Thus, the simplified models provided good estimates while using only half of the terms of the more complicated models.

Conclusions

One effect was not included in the computational analysis, but was noticed in the graphical analysis. The water-to-solids mass ratios varied greatly between gel compositions; often the $SiO_2 \cdot B_2O_3$ values were twice the SiO_2 values for identical trials. Of the four variables studied, pH had the least statistically significant effect. The slight change seen varied with the gel composition as increasing pH resulted in increasing solvent content for SiO_2 gels, but decreasing solvent content for $SiO_2 \cdot B_2O_3$ gels. The valence and concentration variables had effects with nearly equal magnitude, but with different signs. The water-to-solids mass ratios tended to decrease with decreasing valence and increasing normality. The final variable, rinsing, showed a tendency for decreasing solvent content with increasing rinsing.

A mechanistic experiment was planned using the variables found to be significant. Since further testing should investigate the changes due to the borate concentration in the gel, the experiment was designed using five different gel compositions ranging from SiO_2 to $SiO_2 \cdot B_2O_3$. As before, these gels would be placed in a variety of soaking solutions. The pH would be held constant since its statistical effect was small. The lower level of pH was chosen because it produced a slightly more dense SiO_2 gel. The solvent content decreased with decreasing valence and increasing normality. The lowest valence possible was desired, so Na^+ was used for the soaking solutions. To investigate a wider range of concentrations, the mechanistic experiment was designed with eleven different concentrations of NaCl solutions ranging from the tested lower level of 0.0 N to a higher upper level of 2.0 N. Since rinsing produced a more dense gel, all gels in the following test were to be rinsed.

References

[1] Course notes from "Strategy of Experimentation," Dupont Professional Training Seminars, copyright 1974.

[2] Vold, Robert D. and Marjorie J. Vold. Colloid and Interface Chemistry. Reading, Massachusetts: Addison-Wesley Publishing Company, Inc., 1983.

[3] Tanaka, Toyoichi. "Gels," Scientific American, 244: 124-138 (1981).

[4] Hendrix, Charles D. "What Every Technologist Should Know about Experimental Design," Chemtech: 167-174 (March 1979).

[5] Yoldas, B. E. "Monolithic Glass Formation by Chemical Polymerization," Journal of Materials Science, 14: 1843-1849 (1979).

[6] Yamane, Masayuki, et al. "Preparation of a Gel from Metal Alkoxide and its Properties as Precursor of Oxide Glass," Journal of Materials Science, 13: 865-870 (1978).

[7] Nogami, M. and Y. Moriya. "Glass Formation of the SiO_2-B_2O_3 System by the Gel Process from Metal Alkoxides," Journal of Non-Crystalline Solids, 48: 359-366 (1982).

Table 2.1. 2^4 Factorial Design Pattern
with Center Point [1].

Trial	Coded Factors			
	x_1	x_2	x_3	x_4
1	−	−	−	−
2	+	−	−	−
3	−	+	−	−
4	+	+	−	−
5	−	−	+	−
6	+	−	+	−
7	−	+	+	−
8	+	+	+	−
9	−	−	−	+
10	+	−	−	+
11	−	+	−	+
12	+	+	−	+
13	−	−	+	+
14	+	−	+	+
15	−	+	+	+
16	+	+	+	+
17	0	0	0	0

Table 2.2. Two-Level Factorials with a Center Point

Variable	Range of Variable		
	(−)	(0)	(+)
x_1 Electrolyte Valence	Na^+	Mg^{2+}	Al^{3+}
x_2 Concentration	0.0 N	0.5 N	1.0 N
x_3 pH	4 pH	7 pH	10 pH
x_4 Rinsing	No Rinse	Half Rinse	Full Rinse

Response (y) measured in $\frac{\text{mass water}}{\text{mass solid}}$

Table 2.3. Two-Level Factorials with a Center
Point Duplicated and Randomized Design

Order	Trial	Valence (x_1)	Concentration (x_2)	pH (x_3)	Rinsing (x_4)
1	8	Al^{3+}	1.0 N	10	no
2	15	Na^+	1.0 N	10	full
3	14	Al^{3+}	0.0 N	10	full
4	10	Al^{3+}	0.0 N	4	full
5	16	Al^{3+}	1.0 N	10	full
6	13	Na^+	0.0 N	10	full
7	3	Na^+	1.0 N	4	no
8	7	Na^+	1.0 N	10	no
9	4	Al^{3+}	1.0 N	4	no
10	9	Na^+	0.0 N	4	full
11	12	Al^{3+}	1.0 N	4	full
12	6	Al^{3+}	0.0 N	10	no
13	1	Na^+	0.0 N	4	no
14	2	Al^{3+}	0.0 N	4	no
15	5	Na^+	0.0 N	10	no
16	17	Mg^{2+}	0.5 N	7	half
17	11	Na^+	1.0 N	4	full
18	17	Mg^{2+}	0.5 N	7	half
19	10	Al^{3+}	0.0 N	4	full
20	2	Al^{3+}	0.0 N	4	no
21	9	Na^+	0.0 N	4	full
22	17	Mg^{2+}	0.5 N	7	half
23	3	Na^+	1.0 N	4	no
24	11	Na^+	1.0 N	4	full
25	17	Mg^{2+}	0.5 N	7	half
26	1	Na^+	0.0 N	4	no
27	13	Na^+	0.0 N	10	full
28	7	Na^+	1.0 N	10	no
29	12	Al^{3+}	1.0 N	4	full
30	16	Al^{3+}	1.0 N	10	full
31	8	Al^{3+}	1.0 N	10	no
32	6	Al^{3+}	0.0 N	10	no
33	14	Al^{3+}	0.0 N	10	full
34	4	Al^{3+}	1.0 N	4	no
35	5	Na^+	0.0 N	10	no
36	15	Na^+	1.0 N	10	full

Table 2.4. Computational Table for a 2^4 Factorial Experiment [1].

Trial	$\bar{y}$	Mean	x_1	x_2	x_3	x_4	x_1x_2	x_1x_3	x_1x_4	x_2x_3	x_2x_4	x_3x_4	$x_1x_2x_3$	$x_1x_2x_4$	$x_1x_3x_4$	$x_2x_3x_4$	$x_1x_2x_3x_4$
1		+	−	−	−	−	+	+	+	+	+	+	−	−	−	−	+
2		+	+	−	−	−	−	−	−	+	+	+	+	+	+	−	−
3		+	−	+	−	−	−	+	+	−	−	+	+	+	−	+	−
4		+	+	+	−	−	+	−	−	−	−	+	−	−	+	+	+
5		+	−	−	+	−	+	−	+	−	+	−	+	−	+	+	−
6		+	+	−	+	−	−	+	−	−	+	−	−	+	−	+	+
7		+	−	+	+	−	−	−	+	+	−	−	−	+	+	−	+
8		+	+	+	+	−	+	+	−	+	−	−	+	−	−	−	−
9		+	−	−	−	+	+	+	−	+	−	−	−	+	+	+	−
10		+	+	−	−	+	−	−	+	+	−	−	+	−	−	+	+
11		+	−	+	−	+	−	+	−	−	+	−	+	−	+	−	+
12		+	+	+	−	+	+	−	+	−	+	−	−	+	−	−	−
13		+	−	−	+	+	+	−	−	−	−	+	+	+	−	−	+
14		+	+	−	+	+	−	+	+	−	−	+	−	−	+	−	−
15		+	−	+	+	+	−	−	−	+	+	+	−	−	−	+	−
16		+	+	+	+	+	+	+	+	+	+	+	+	+	+	+	+

sum+ =

sum− =

overall sum =

Difference =

Effect =

(Trial 17) Center Point Average =   Curvature =   [min] =   [min C] =

Table 2.5. Computational Analysis of SiO$_2$.

Trial	$\bar{y}$	Mean	x_1	x_2	x_3	x_4	x_1x_2	x_1x_3	x_1x_4	x_2x_3	x_2x_4	x_3x_4	$x_1x_2x_3$	$x_1x_2x_4$	$x_1x_3x_4$	$x_2x_3x_4$	$x_1x_2x_3x_4$
1	1.467	+	-	-	-	-	+	+	+	+	+	+	-	-	-	-	+
2	1.346	+	+	-	-	-	-	-	-	+	+	+	+	+	+	-	-
3	1.114	+	-	+	-	-	-	+	+	-	-	+	+	+	-	+	-
4	1.513	+	+	+	-	-	+	-	-	-	-	+	-	-	+	+	+
5	1.627	+	-	-	+	-	+	-	+	-	+	-	+	-	+	+	-
6	1.781	+	+	-	+	-	-	+	-	-	+	-	-	+	-	+	+
7	1.142	+	-	+	+	-	-	-	+	+	-	-	-	+	+	-	+
8	1.388	+	+	+	+	-	+	+	-	+	-	-	+	-	-	-	-
9	1.527	+	-	-	-	+	+	+	-	+	-	-	-	+	+	+	-
10	1.608	+	+	-	-	+	-	-	+	+	-	-	+	-	-	+	+
11	1.337	+	-	+	-	+	-	+	-	-	+	-	+	-	+	-	+
12	1.636	+	+	+	-	+	+	-	+	-	+	-	-	+	-	-	-
13	1.601	+	-	-	+	+	+	-	-	-	-	+	+	+	-	-	+
14	1.488	+	+	-	+	+	-	+	+	-	-	+	-	-	+	-	-
15	1.429	+	-	+	+	+	-	-	-	+	+	+	-	-	-	+	-
16	1.682	+	+	+	+	+	+	+	+	+	+	+	+	+	+	+	+

		sum+ = 23.686	12.442	11.241	12.138	12.308	12.441	11.784	11.764	11.589	12.305	11.640	11.703	11.829	11.662	12.281	12.131
		sum- = 0.000	11.244	12.445	11.548	11.378	11.245	11.902	11.922	12.097	11.381	12.046	11.983	11.857	12.024	11.405	11.555
		overall sum = 23.686	23.686	23.686	23.686	23.686	23.686	23.686	23.686	23.686	23.686	23.686	23.686	23.686	23.686	23.686	23.686
Difference = 23.686			1.198	-1.204	0.590	0.930	1.196	-0.118	-0.158	-0.508	0.924	-0.406	-0.280	-0.028	-0.362	0.879	0.576
Effect = 1.480			0.150 *	-0.150 *	0.074	0.116 *	0.150 *	-0.015	-0.020	-0.064	0.116 *	-0.051	-0.035	-0.004	-0.045	0.110 *	0.072

(Trial 17) Center Point Average = 1.386

Curvature = 1.480 - 1.386 = 0.094   [min] = 0.100   [min C] = 0.150

Table 2.6. Computational Analysis of $SiO_2 \cdot B_2O_3$.

Trial	$\bar{y}$	Mean	x_1	x_2	x_3	x_4	x_1x_2	x_1x_3	x_1x_4	x_2x_3	x_2x_4	x_3x_4	$x_1x_2x_3$	$x_1x_2x_4$	$x_1x_3x_4$	$x_2x_3x_4$	$x_1x_2x_3x_4$
1	2.950	+	−	−	−	−	+	+	+	+	+	+	−	−	−	−	+
2	2.926	+	+	−	−	−	−	−	−	+	+	+	+	+	+	−	−
3	2.214	+	−	+	−	−	−	+	+	−	−	+	+	+	−	+	−
4	2.577	+	+	+	−	−	+	−	−	−	−	+	−	−	+	+	+
5	2.237	+	−	−	+	−	+	−	+	−	+	−	+	−	+	+	−
6	2.475	+	+	−	+	−	−	+	−	−	+	−	−	+	−	+	+
7	1.809	+	−	+	+	−	−	−	+	+	−	−	−	+	+	−	+
8	2.421	+	+	+	+	−	+	+	−	+	−	−	+	−	−	−	−
9	3.194	+	−	−	−	+	+	+	−	+	−	−	−	+	+	+	−
10	3.280	+	+	−	−	+	−	−	+	+	−	−	+	−	−	+	+
11	2.990	+	−	+	−	+	−	+	−	−	+	−	+	−	+	−	+
12	3.166	+	+	+	−	+	+	−	+	−	+	−	−	+	−	−	−
13	3.424	+	−	−	+	+	+	−	−	−	−	+	+	+	−	−	+
14	3.259	+	+	−	+	+	−	+	+	−	−	+	−	−	+	−	−
15	2.340	+	−	+	+	+	−	−	−	+	+	+	−	−	−	+	−
16	3.496	+	+	+	+	+	+	+	+	+	+	+	+	+	+	+	+
sum+ =	44.758		23.600	21.013	21.461	25.149	23.465	22.999	22.411	22.416	22.580	23.186	22.988	22.704	22.488	21.813	23.001
sum− =	0.000		21.158	23.745	23.297	19.609	21.293	21.759	22.347	22.342	22.178	21.572	21.770	22.054	22.270	22.945	21.757
overall sum =	44.758		44.758	44.758	44.758	44.758	44.758	44.758	44.758	44.758	44.758	44.758	44.758	44.758	44.758	44.758	44.758
Difference =	44.758		2.442	−2.732	−1.836	5.540	2.172	1.240	0.064	0.074	0.402	1.614	1.218	0.650	0.218	−1.132	1.244
Effect =	2.797		0.305	−0.342	−0.230	0.693	0.272	0.155	0.008	0.009	0.050	0.202	0.152	0.081	0.027	−0.142	0.156

(Trial 17) Center Point Average = 2.896

Curvature = 2.797 − 2.896 = −0.099   [min] = 0.372   [min C] = 0.558

Table 2.7. Comparison of SiO_2 Models for Sixteen Design Points

Trial	$\bar{y}$ Actual Response Value	$\hat{y}$ Eqn. 2.6 Predicted Response Value	$\frac{\bar{y} - \hat{y}}{\bar{y}} \times 100\%$ Normalized Difference	$\hat{y}$ Eqn. 2.7 Predicted Response Value	$\frac{\bar{y} - \hat{y}}{\bar{y}} \times 100\%$ Normalized Difference
1	1.467	1.466	0.0682	1.500	−2.249
2	1.346	1.345	0.0743	1.500	−11.441
3	1.114	1.113	0.0898	1.194	−7.181
4	1.513	1.514	−0.0660	1.494	1.256
5	1.627	1.628	−0.0615	1.610	1.045
6	1.781	1.781	0.0000	1.610	9.601
7	1.142	1.141	0.0876	1.084	5.079
8	1.388	1.388	0.0000	1.384	0.288
9	1.527	1.526	0.0655	1.610	−5.435
10	1.608	1.607	0.0622	1.610	−0.124
11	1.337	1.337	0.0000	1.316	1.571
12	1.636	1.636	0.0000	1.616	1.222
13	1.601	1.600	0.0625	1.500	6.309
14	1.488	1.487	0.0672	1.500	−0.806
15	1.429	1.429	0.0000	1.426	0.210
16	1.682	1.682	0.0000	1.726	−2.616

Table 2.8. Comparison of $SiO_2 \cdot B_2O_3$ Models for Sixteen Design Points

Trial	$\bar{y}$ Actual Response Value	$\hat{y}$ Eqn. 2.8 Predicted Response Value	$\frac{\bar{y} - \hat{y}}{\bar{y}} \times 100\%$ Normalized Difference	y Eqn. 2.10 Predicted Response Value	$\frac{\bar{y} - \hat{y}}{\bar{y}} \times 100\%$ Normalized Difference
1	2.950	2.951	−0.0339	2.821	4.373
2	2.926	2.925	0.0342	2.854	2.461
3	2.214	2.213	0.0452	2.207	0.316
4	2.577	2.577	0.0000	2.784	−8.033
5	2.237	2.236	0.0447	2.389	−6.795
6	2.475	2.474	0.0404	2.422	2.141
7	1.809	1.808	0.0553	1.775	1.879
8	2.421	2.420	0.0413	2.352	2.850
9	3.194	3.194	0.0000	3.312	−3.694
10	3.280	3.280	0.0000	3.345	−1.982
11	2.990	2.990	0.0000	2.698	9.766
12	3.166	3.166	0.0000	3.275	−3.443
13	3.424	3.425	−0.0292	3.284	4.089
14	3.259	3.259	0.0000	3.317	−1.780
15	2.340	2.339	0.0427	2.670	−14.103
16	3.496	3.495	0.0286	3.247	7.122

(a) 2^4 Factorial Design

(b) Factor Effect x_1

(c) Interaction $x_1 x_2$

(d) Interaction $x_1 x_2$

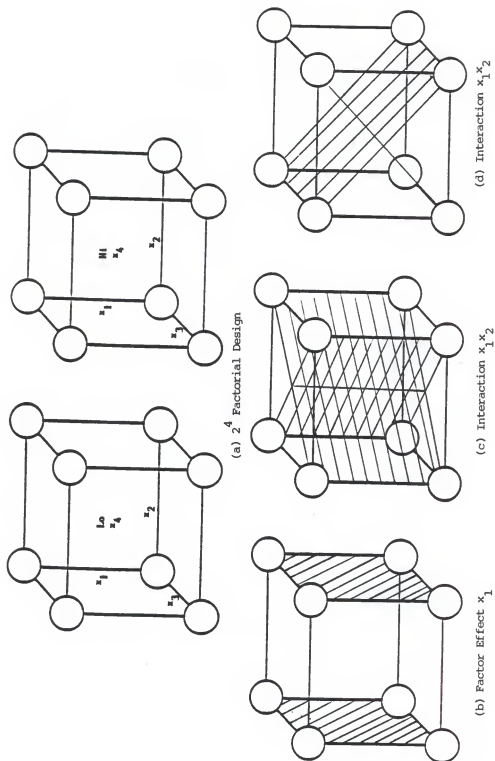Figure 2.1. Factorial Geometry.
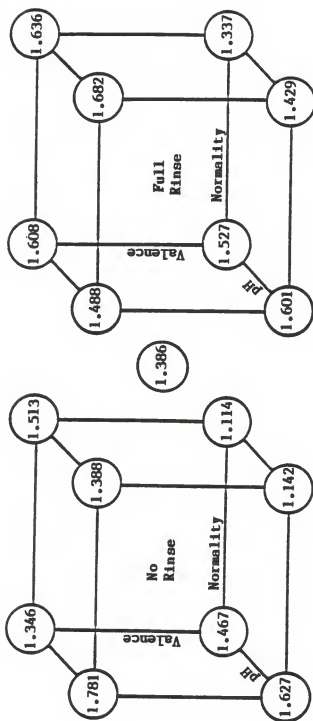
Figure 2.2. Water-to-Solids Mass Ratios for SiO_2.

36
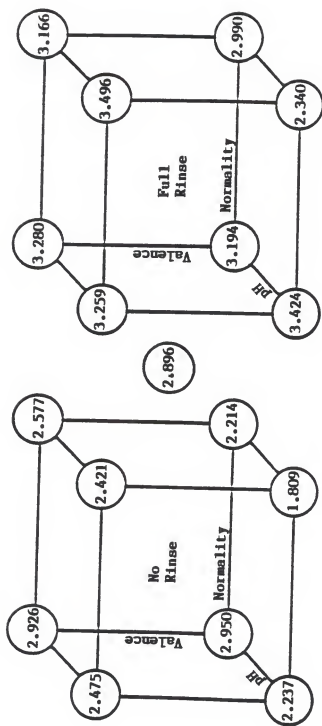
Figure 2.3. Water-to-Solids Mass Ratios for $SiO_2 \cdot B_2O_3$.

III. The Mechanistic Experiment

Background

The information provided by the 2^4 factorial experiment was used to identify important variables and their effects on the solvent content of the gel. The solvent variables investigated were electrolyte valence, electrolyte concentration and pH, while the gel preparation variables were composition and rinsed state. Graphical and computational analyses were conducted to determine how these variables influenced the water-to-solids mass ratio and with this knowledge, a more detailed, mechanistic experiment was planned. The objective of this experiment was to produce a more dense gel as reflected in a lower solvent content. The magnitude of the variations in the water-to-solids mass ratios due to gel composition were on an order larger than the changes associated with the other variables. The $SiO_2 \cdot B_2O_3$ values were twice the SiO_2 values for identical trials. Thus, a more extensive investigation of the effect of the borate concentration in the gel was warranted. The valence and concentration variables had effects of similar magnitude, but of opposite direction. The water-to-solids mass ratio decreased with decreasing valence and increasing normality. The changes due to pH were not statistically significant. Finally, the rinsed gels yielded lower solvent content than the unrinsed gels.

The resulting mechanistic experiment included five different gel compositions: SiO_2, $SiO_2 \cdot \frac{1}{4}B_2O_3$, $SiO_2 \cdot \frac{1}{2}B_2O_3$, $SiO_2 \cdot \frac{3}{4}B_2O_3$ and $SiO_2 \cdot B_2O_3$. The lowest valence possible was desired, so Na^+ was used for the soaking solutions. A wider range of electrolyte concentration was needed and eleven different NaCl solutions with concentrations ranging from 0.0 N to 2.0 N were used. Since the effect of pH was not significant, it was held constant in these experiments. A pH of 4 was chosen since it produced a

slightly more dense SiO_2 gel. Because the rinsed gels had lower water-to-solids mass ratios, all gels were rinsed.

Experimental Procedure

Five compositions of rinsed borosilicate gels were studied in eleven concentrations of NaCl solutions, each at a pH of 4. At least one mass water/mass solids measurement was conducted at each combination of composition and concentration. Specific volume measurements were also made. These two response evaluation techniques measured different properties of the gel although both characterized volume changes. Replicate samples were prepared so that confidence intervals could be established for both the water-to-solids mass ratios and the specific volume results. The number of data points at each condition is given in Tables 3.1 through 3.5.

Borosilicate Gel Synthesis. The experimental procedure used for making borosilicate gels was the same as that used for the designed experiment except for the changes below.

(1) In order to have better control over the gel composition during synthesis, the synthesis was conducted in a closed 3-necked, round-bottom flask. The center arm was fitted with a plastic stirring rod. One side arm was fitted with a condenser. The other side arm was used when the reactants were added to the flask. During the reaction, this was closed with a glass stopper. This system greatly reduced the loss of the reactants and products due to vaporization. The loss of trimethyl borate was of particular concern since this chemical was the most volatile of those used in the synthesis.

(2) The amount of $B(OCH_3)_3$ added in the synthesis procedure was

calculated for the new compositions. The quantities used are listed below:

Gel Type	$B(OCH_3)_3$ Added
SiO_2	none
$SiO_2 \cdot \frac{1}{4}B_2O_3$	11 ± 0.5 ml
$SiO_2 \cdot \frac{1}{2}B_2O_3$	23 ± 0.5 ml
$SiO_2 \cdot \frac{3}{4}B_2O_3$	34 ± 0.5 ml
$SiO_2 \cdot B_2O_3$	45 ± 0.5 ml

(3) The volume of the liquid gel produced was measured before it was distributed into the 50 ml polypropylene beakers. If the final volume of a batch was less than that expected for that gel type, the gel samples produced were not used. A difference as small as 5% meant that the evaporative losses were too large, making the actual gel composition inconsistent with other batches. Once the gel was poured out in 8 ml portions, the beakers were closed with number 10 size polypropylene stoppers as these were found to seal better than the Parafilm used earlier. This reduced borate losses before gelation.

(4) Once the gels were removed from the beakers, they were sliced into four equal size samples. Gel samples of identical compositions were placed in an air tight container with a 50% water/50% ethanol solution. A pump with a system of inlet, outlet and reflux tubing was used to gradually replace the solution with deionized water (Figure 3.1). The ethanol content of the outlet stream was determined from its refractive index. The rinsing continued until the exiting solution was at least 99% water. Then the rinsed gel

sections were placed into the electrolyte solution desired. The
containers were sealed as before and set aside for four weeks.

Response Evaluation. The water-to-solids mass ratio was measured with
the same loss on dehydration procedure used for the 2^4 factorial experiment
(LOD/110°C). Separate gel samples were used to make specific volume
measurements. This analysis was conducted using a pycnometer and the ASTM
standard test method D70 (see Appendix C). This procedure was developed
for specific gravity and density measurements of semi-solid bituminous
materials. The only change necessary in the ASTM procedure was to use
the appropriate NaCl solutions instead of pure water when filling the
pycnometer. The technique involved determining the weight of the empty
pycnometer, the weight of the pycnometer filled with the solution, the
weight of the pycnometer partially filled with the gel sample and the
weight of the pycnometer plus the gel sample and solution. These values
were used to calculate the specific volume of the gel.

Replicate results from both techniques were handled in the same
manner. When more than one response value was obtained for a particular
set of experimental conditions, the average was reported. Then 95% con-
fidence intervals were calculated using the pooled standard deviation and
a double sided t-distribution [1].

Experimental Results

The water-to-solids mass ratios and specific volume results are listed
in Tables 3.1 through 3.5.

The water-to-solids mass ratio data for all five gel compositions are
presented in Figure 3.2. This plot shows that the water content of the
gels decreased with increasing electrolyte concentration of the solution

and decreasing borate content of the gel. The effect appeared to be linear for low borate concentrations and non-linear for higher borate concentrations. Also, the higher the borate content of the gel, the greater the decrease in liquid-to-solids mass ratio with increasing electrolyte concentration. The complete elimination of borate from the gel composition results in the most dense gels. However, if borate is desired for its material properties, some of the volume increase which results could be corrected for if a high electrolyte concentration solution is used to enhance syneresis.

The $SiO_2 \cdot \frac{1}{2}B_2O_3$ and $SiO_2 \cdot \frac{3}{4}B_2O_3$ results were identical. It is possible that the corrections made to better control the gel composition in the gel production were not sufficient. If the intended borate concentrations were not maintained throughout the synthesis and gelation processes, the actual compositions of the gels would be different than the compositions as batched. Thus the gels produced may not be $SiO_2 \cdot \frac{1}{2}B_2O_3$ and $SiO_2 \cdot \frac{3}{4}B_2O_3$, but rather compositions much more similar to one another. However, the liquid gel volumes which were measured after synthesis and before gelation do not support this assumption. The volumes of the two $SiO_2 \cdot \frac{1}{2}B_2O_3$ gel batches were within 5% of each other as were the volumes of the two $SiO_2 \cdot \frac{3}{4}B_2O_3$ gel batches. In addition, the difference between the measured $SiO_2 \cdot \frac{3}{4}B_2O_3$ yields and the $SiO_2 \cdot \frac{1}{2}B_2O_3$ yields was similar to the difference in the volumes of trimethyl borate added during synthesis. An accurate analysis of the resulting gel compositions is needed to interpret the similarities in the results for these two gel compositions.

The water-to-solids mass ratio as determined did not account for the electrolyte in the solution that was left behind as the water evaporated. Thus, the mass of the water represented only a part of the actual mass of

the solution, while the mass of the solids included the mass of the salt from the solution in addition to the mass of the dried borosilicate gels. These factors result in a lower water-to-solids mass ratio and the magnitude of the change increased with increasing electrolyte concentration. The salt originally present in the amount of water that was evaporated from the gel was calculated assuming the solution in the wet gel contained the same electrolyte concentration as the bulk solution. This value was added to the mass water to estimate the mass solvent and subtracted from the mass solids to approximate the mass $SiO_2 \cdot xB_2O_3$. Thus, the mass ratio so defined includes a correction for the salt content in the electrolyte solution. These values are listed in Tables 3.1 through 3.5 and are plotted in Figure 3.3. This correction reduced the overall change in the solvent content due to increasing electrolyte concentration. However, more dense gels are being produced as the solvent-to-$SiO_2 \cdot xB_2O_3$ mass ratios still decreased with increasing electrolyte concentration.

The specific volume results are plotted in Figure 3.4. There was a slight decrease in specific volume with increasing electrolyte concentration which was consistent with the liquid-to-solids mass ratio results. The change in the gel volumes due to the gel composition also matched the previous results as the volumes increased with increasing borate content. The error bars range from 2% to 9% and account for the scatter seen in Figure 3.4. The specific volume technique had many sources of error. Four weighings were necessary for each data point and any errors were compounded in the calculations. These measurements were affected by the precision of the balance (10^{-3} grams), air bubbles in the pycnometer, and changes in temperature due to continued handling. The small sample size was also a factor (the mass of the gel samples were less than one gram). Although all

samples were blotted in the same manner, their "wet" weights were influenced by the amount of surface water present when they were removed from the soaking solutions. Future specific volume measurements should include larger gel samples and more precise mass measurements so that the magnitude of these errors can be minimized.

Discussion

A gel will expand or contract according to the total of the forces acting upon it. These combined forces are called the osmotic pressure and, whenever possible, the gel will adapt its volume so that the total osmotic pressure is zero. When the pressure is positive, an unrestrained gel will swell taking up excess fluid if it is available. When the pressure is negative, the gel eliminates fluid and shrinks. The swelling or shrinking continues until the different positive and negative forces exactly cancel one another and the gel is at equilibrium.

In his work with hydrolyzed polyacrylamide gel phase transitions, Tanaka identifies three of the forces which make up the osmotic pressure: the rubber elasticity, the polymer-polymer affinity and the hydrogen-ion pressure [3]. Tanaka begins with Flory's formula [4] for osmotic pressure, which follows below.

$$\pi = -RT\left[\ln(1 - \phi) + \phi + \frac{\theta}{2T}\phi^2 + \nu_o\left(\frac{\phi}{\phi_o}\right)^{1/3} - \nu_o\frac{\phi}{2\phi_o}\right] \tag{3.1}$$

where

R = gas constant

T = absolute temperature

ϕ = volume fraction occupied by the network in the gel after the
    volume change

ϕ_o = volume fraction of uncrosslinked single polymer chain in absence of interaction among segments in chain

θ = theta temperature [4]

$\nu_o = n_o \nu_o$

n_o = number of crosslinks per volume of gel with volume fraction $\phi = \phi_o$

ν_o = effective volume of each crosslink unit

The first two terms represent the entropy, the third term the enthalpy of mixing of the polymer network and the fluid, and the last two terms the excess rubber elasticity of the network due to volume changes of the gel. Since Tanaka's experiments involved the condition of $\phi \ll 1$, he expanded the first term to produce the following equation [5].

$$\pi \simeq RT\phi_o^3 \left[\frac{1}{2\phi_o} \left(1 - \frac{\theta}{T} \right) \rho^2 + \frac{\rho^3}{3} + S \left(\frac{\rho}{2} - \rho^{1/3} \right) \right] \tag{3.2}$$

where

$\rho \equiv \dfrac{\phi}{\phi_o}$

$S \equiv \dfrac{\nu_o}{\phi_o^3}$ for $\phi \ll 1$

This condition may be applicable to this work with borosilicate gels as well. Tanaka presented swelling data for varying degrees of hydrolysis as a function of the composition, temperature, pH and electrolyte concentration of the solvent and the voltage gradient across the gel [3,5,6]. He found that dissolved salts can collapse a gel since the sodium ions shield the negative charges of the polymer, while the chloride ions neutralize the hydrogen ions. This decreases the effective ionization of the polymer which reduces the osmotic pressure, promoting syneresis. Since equation 3.2 does not consider the distribution of the salt, another

approach is needed in developing an equation to better describe the situation.

The Donnan equilibrium is the particular situation which occurs when two coexisting phases are restricted such that one or more of the ionic components cannot pass from one phase into the other. This restriction is often caused by a membrane which is permeable to the solvent and low molecular weight ions but impermeable to colloidal electrolyte or charged particles of higher molecular weight. The Donnan equilibrium states that the products of the activities of the positive and negative ions on both sides of the membrane are equal. This statement of equilibrium can be used to develop an expression for the osmotic pressure of a system consisting of a solvent, a colloidal electrolyte and a low molecular weight 1:1 electrolyte [7].

$$\pi = \frac{M_1 RT}{1000 V_1^{\circ}} \left[(1 + z)m_P + 2m_M - 2m_M \left(1 + \frac{zm_P}{m_M} \right)^{1/2} \right] \tag{3.3}$$

where

  M = molecular weight of solvent

  V_1° = volume of solvent

  z = valence number of positively charged colloidal ions

  m_P = moles colloidal electrolyte per kilogram solvent

  m_M = moles solute electrolyte per kilogram solvent

The two extreme values of m_M include the conditions of no added electrolyte, $m_M = 0$, and "swamping" by the electrolyte, $m_M \gg m_P$. These special cases are presented below, where m_P is in moles kg^{-1} [7].

$$\pi = \frac{M_1 RT}{1000 V_1^{\circ}} (1 + z)m_P \qquad\qquad m_M = 0 \tag{3.4}$$

$$\pi = \frac{M_1 RT}{1000V_1} m_P \qquad\qquad m_M \gg m_P \qquad (3.5)$$

Although these equations were developed for the case of a semipermeable membrane, they can be applied to a colloidal system. In fact, the colloidal system itself can be viewed as a membrane. The continuous phase acts as the solid portion of the membrane while the dispersed phase behaves like the pores of the membrane. Equations 3.4 and 3.5 show that the osmotic pressure is higher at the condition of no added electrolyte than when there is swamping by the electrolyte. The lower osmotic pressure under the second condition means that a gel will expel fluid and shrink when placed in a high concentration of electrolyte. This was precisely the behavior seen with the water-to-solids mass ratio and specific volume results.

Tanaka observed abrupt changes in the gel volumes which he attributed to phase transitions [3,5,6]. Although the change in the solvent content with increasing electrolyte concentration was non-linear at the higher borate concentration, the borosilicate gels did not appear to exhibit a phase transition like that of the polyacrylamide gels. In addition, the solvent-to-$SiO_2 \cdot xB_2O_3$ mass ratios behaved linearly with respect to electrolyte concentration at all borate concentrations. Perhaps the various forces that make up the osmotic pressure in the borosilicate gels respond differently to the increase in electrolyte concentration, the combined effect being a smooth curve.

Conclusions

The mechanistic experiment investigated the variables found to be significant in the 2^4 factorial design experiment. Five compositions of rinsed borosilicate gels were studied in eleven concentrations of NaCl

solutions, each at a pH of 4. The results showed a decrease in the water content of the gels with increasing electrolyte concentration of the solution and decreasing borate content of the gel. The effect appeared to be linear for low borate concentrations and non-linear for higher borate concentrations. A correction for the salt content in the electrolyte solution reduced the gel volume change due to the electrolyte concentration, but the effect was still real. Specific volume measurements were also conducted which were consistent with the previous results in that the gel volumes decreased with increasing electrolyte concentration and decreasing borate content of the gel. These volume changes were described in terms of the osmotic pressure and Donnan equilibrium.

References

[1] Course notes from "Strategy of Experimentation," Dupont Professional Training Seminars, copyright 1974.

[2] Vold, Robert D. and Marjorie J. Vold. _Colloid and Interface Chemistry_. Reading, Massachusetts: Addison-Wesley Publishing Company, Inc., 1983.

[3] Tanaka, Toyoichi. "Gels," _Scientific American_, 244: 124-138 (1981).

[4] Flory, P. J. _Principles of Polymer Chemistry_. Ithaca, New York: Cornell University Press, 1953.

[5] Tanaka, Toyoichi. "Collapse of Gels and the Critical Endpoint," _Physical Review Letters_, 40: 820-823 (1978).

[6] Tanaka, Toyoichi, _et al_. "Phase Transitions in Ionic Gels," _Physical Review Letters_, 45: 1636-1639 (1980).

[7] Hiemenz, Paul C. _Principle of Colloid and Surface Chemistry_. New York: Marcel Dekker, Inc., 1977.

Table 3.1. Results for SiO$_2$ Gels.

Sample Solution	Number of $\frac{\text{Mass Water}}{\text{Mass Solids}}$ Samples	$\frac{\text{Mass Water}}{\text{Mass Solids}}$	$\frac{\text{Mass Solvent}}{\text{Mass SiO}_2 \cdot x\text{B}_2\text{O}_3}$	Number of Specific Volume Samples	Specific Volume (ml/g)
2.0 N	2	1.155 ± 0.5	1.377	3	0.729 ± 0.03
1.8 N	1	1.309	1.546	1	0.749
1.6 N	1	1.307	1.516	1	0.762
1.4 N	1	1.173	1.327	1	0.711
1.2 N	1	1.225	1.365	1	0.695
1.0 N	3	1.299 ± 0.4	1.427	3	0.758 ± 0.03
0.8 N	1	1.333	1.438	1	0.694
0.6 N	1	1.796	1.925	1	0.793
0.4 N	1	1.041	1.076	1	0.737
0.2 N	1	1.119	1.138	1	0.754
0.0 N	3	1.690 ± 0.4	1.690	3	0.754 ± 0.03

Table 3.2. Results for $SiO_2 \cdot \frac{1}{4}B_2O_3$ Gels.

Sample Solution	Number of $\frac{\text{Mass Water}}{\text{Mass Solids}}$ Samples	$\frac{\text{Mass Water}}{\text{Mass Solids}}$	$\frac{\text{Mass Solvent}}{\text{Mass } SiO_2 \cdot xB_2O_3}$	Number of Specific Volume Samples	Specific Volume (ml/g)
2.0 N	3	1.895 ± 0.4	2.412	3	0.832 ± 0.05
1.8 N	2	1.803 ± 0.5	2.220	1	0.791
1.6 N	2	1.949 ± 0.5	2.368	1	0.835
1.4 N	2	2.303 ± 0.5	2.828	1	0.791
1.2 N	2	2.022 ± 0.5	2.349	1	0.808
1.0 N	3	2.490 ± 0.4	2.881	3	0.832 ± 0.05
0.8 N	2	2.243 ± 0.5	2.498	1	0.851
0.6 N	2	2.299 ± 0.5	2.497	1	0.861
0.4 N	2	2.376 ± 0.5	2.513	1	0.808
0.2 N	2	1.878 ± 0.5	1.924	1	0.782
0.0 N	3	2.460 ± 0.4	2.460	3	0.840 ± 0.05

Table 3.3. Results for $SiO_2 \cdot \frac{1}{2}B_2O_3$ Gels.

Sample Solution	Number of Mass Water Mass Solids Samples	$\dfrac{\text{Mass Water}}{\text{Mass Solids}}$	$\dfrac{\text{Mass Solvent}}{\text{Mass SiO}_2 \cdot x\text{B}_2\text{O}_3}$	Number of Specific Volume Samples	Specific Volume (ml/g)
2.0 N	6	2.558 ± 0.4	3.463	6	0.862 ± 0.04
1.8 N	2	2.610 ± 0.7	3.438	2	0.779 ± 0.07
1.6 N	3	2.684 ± 0.6	3.505	2	0.801 ± 0.07
1.4 N	3	2.871 ± 0.6	3.615	2	0.820 ± 0.07
1.2 N	2	3.059 ± 0.7	3.762	2	0.772 ± 0.07
1.0 N	6	2.829 ± 0.4	3.342	6	0.806 ± 0.04
0.8 N	2	3.111 ± 0.7	3.576	2	0.813 ± 0.07
0.6 N	3	3.140 ± 0.6	3.491	2	0.870 ± 0.07
0.4 N	3	3.338 ± 0.6	3.591	2	0.828 ± 0.07
0.2 N	2	3.553 ± 0.7	3.689	2	0.873 ± 0.07
0.0 N	6	3.765 ± 0.4	3.765	6	0.862 ± 0.04

Table 3.4. Results for $SiO_2 \cdot \frac{3}{4} B_2 O_3$ Gels.

Sample Solution	Number of $\frac{\text{Mass Water}}{\text{Mass Solids}}$ Samples	$\frac{\text{Mass Water}}{\text{Mass Solids}}$	$\frac{\text{Mass Solvent}}{\text{Mass } SiO_2 \cdot x B_2 O_3}$	Number of Specific Volume Samples	Specific Volume (ml/g)
2.0 N	5	2.409 ± 0.1	3.209	5	0.852 ± 0.02
1.8 N	3	2.663 ± 0.2	3.528	2	0.782 ± 0.03
1.6 N	3	2.641 ± 0.2	3.381	2	0.815 ± 0.03
1.4 N	3	2.787 ± 0.2	3.487	2	0.836 ± 0.03
1.2 N	3	2.953 ± 0.2	3.612	2	0.838 ± 0.03
1.0 N	5	3.000 ± 0.1	3.554	5	0.868 ± 0.02
0.8 N	3	3.039 ± 0.2	3.481	2	0.860 ± 0.03
0.6 N	3	3.123 ± 0.2	3.465	2	0.870 ± 0.03
0.4 N	3	3.319 ± 0.2	3.567	2	0.863 ± 0.03
0.2 N	3	3.514 ± 0.2	3.649	2	0.874 ± 0.03
0.0 N	5	3.983 ± 0.1	3.983	5	0.877 ± 0.02

Table 3.5. Results for $SiO_2 \cdot B_2O_3$ Gels.

| Sample Solution	Number of $\frac{\text{Mass Water}}{\text{Mass Solids}}$ Samples	$\frac{\text{Mass Water}}{\text{Mass Solids}}$	$\frac{\text{Mass Solvent}}{\text{Mass } SiO_2 \cdot xB_2O_3}$	Number of Specific Volume Samples	Specific Volume (ml/g)
2.0 N	6	3.223 ± 0.6	4.674	6	0.924 ± 0.03
1.8 N	2	3.240 ± 1.0	4.518	2	0.889 ± 0.05
1.6 N	2	3.962 ± 1.0	5.649	2	0.870 ± 0.05
1.4 N	2	3.760 ± 1.0	5.075	2	0.853 ± 0.05
1.2 N	2	4.080 ± 1.0	5.362	2	0.873 ± 0.05
1.0 N	6	3.986 ± 0.6	4.965	6	0.906 ± 0.03
0.8 N	2	4.105 ± 1.0	4.888	2	0.875 ± 0.05
0.6 N	2	4.391 ± 1.0	5.072	2	0.894 ± 0.05
0.4 N	2	5.338 ± 1.0	5.952	2	0.904 ± 0.05
0.2 N	2	5.231 ± 1.0	5.525	2	0.907 ± 0.05
0.0 N	6	4.976 ± 0.6	4.976	6	0.914 ± 0.03
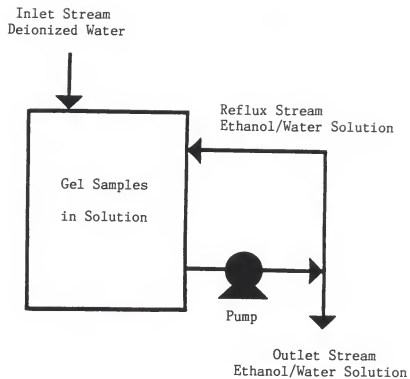
Figure 3.1. Schematic Diagram Showing System of Inlet, Outlet, and Reflux Tubing Used to Rinse Gel Samples.
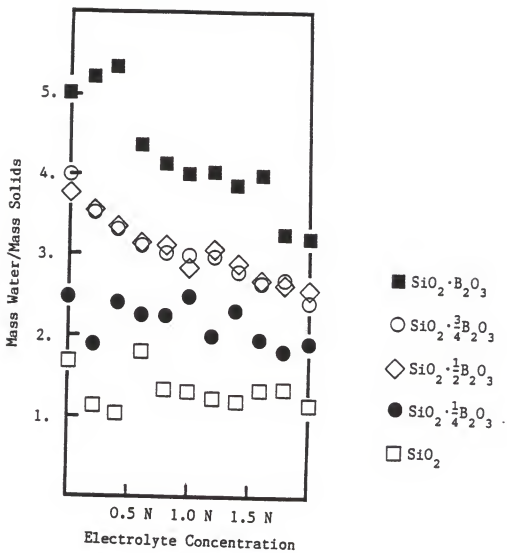
Figure 3.2. Water-to-Solids Mass Ratios.
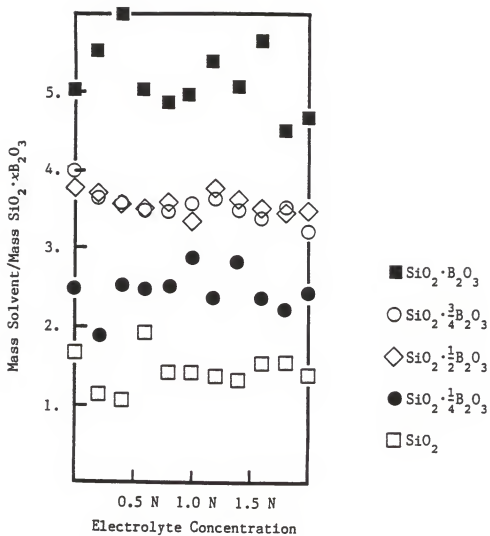
Figure 3.3. Solvent-to-SiO$_2 \cdot x$B$_2$O$_3$ Mass Ratios.
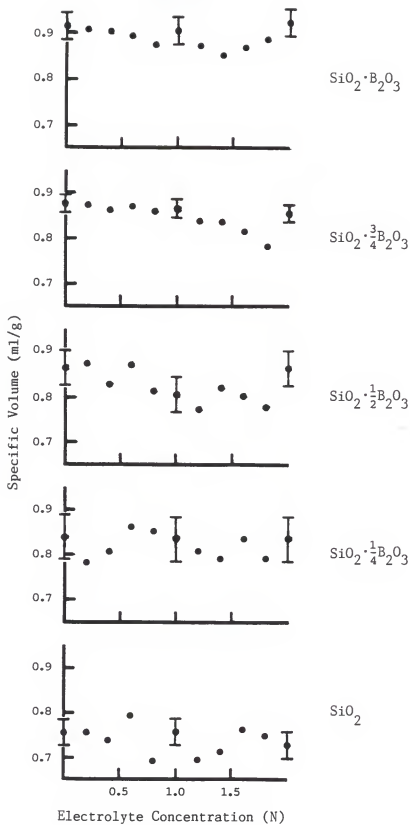
Figure 3.4. Specific Volume Results.

IV. <u>Development</u> <u>of</u> <u>a</u> <u>Negative</u> <u>Adsorption</u> <u>Procedure</u>

Background

The major disadvantage of the sol-gel techniques used to prepare
ceramic materials is the large, uncontrolled shrinkage of the gel during
the drying and sintering processes [1]. Lengthy drying times are required
to minimize the internal stresses caused by the volume changes on drying
and the capillary forces in the gel pores [2]. The research presented in
the previous chapters sought to reduce the problems associated with the
drying process by first minimizing the gel volumes in the wet state. One
measure of the effectiveness of this induced syneresis is the volume change
of the gels as discussed earlier. Another measure of that change would
be the specific surface area of the gels. This chapter concerns the
development of a negative adsorption procedure capable of measuring the
surface areas of wet gels.

Negative adsorption was the approach chosen for the specific surface
area determination since this technique requires that the gel samples
remain in solution. Dry surface area measurements, such as the BET tech-
nique based upon gas adsorption, would not accurately reflect the pore
conditions in the wet state since the gels usually collapse when dried [3].
With other wet methods, such as dye adsorption, there is uncertainty about
the size, configuration and orientation of the adsorbing dye molecule.
Also, the relatively large dye molecules are attached to specific sites
in accessible areas of the samples. Therefore, the area measured with a
dye is likely to be less than that available to smaller ions, such as H_3O^+
[4]. Negative adsorption can be used to determine the specific surface
areas of suspended charged particles without knowledge of the adsorbing
molecule or ion's size. In addition, the measurements are made using

electrolyte solutions such as the NaCl solutions used elsewhere in this investigation.

Theory

In a system consisting of a charged particle with the surrounding solution, counterions are drawn towards the interface of the particle and away from the bulk phase. This accumulation at the interface is called positive adsorption, or simply adsorption. At the same time, co-ions with the same electrical charge as the particle surface are repelled into the bulk solution; that is, they are negatively adsorbed. This causes an increase in the bulk concentration of co-ions. Since the magnitude of this increase in concentration reflects the number of co-ions repelled by the surface, the change in concentration is proportional to the charge density, and therefore, the surface area of the charged particle. Diffuse double-layer theory provides the proportionality constant which relates the increase in the bulk concentration to the surface area. The van den Hul and Lyklema approach considers the distribution of ions about a central particle in both the presence and the absence of a surface charge [5]. A general expression is derived assuming a Boltzmann distribution for the concentration of the negatively adsorbed co-ions with respect to the surface. This equation is simplified by the assumption that only one electrolyte is present. In addition, the potential at the surface, ψ_o, is defined as $-\infty$, which means that the concentration of expelled anions close to the negative surface is zero. The van den Hul and Lyklema equation for surface area follows.

$$S = V_t \frac{\Delta C_1 \kappa}{C_1 A'} \qquad (4.1)$$

where

S = Surface area (cm^2)

V_t = Total volume of solution (cm^3)

C_1 = Equilibrium concentration of negatively adsorbed ions (gram ions/cm^3)

ΔC_1 = Increase in concentration of bulk solution

$1/A'$ = Solution of the integral in the general equation before simplification [5]

$\kappa = \left(\dfrac{4\pi e^2 N}{\varepsilon kT} \sum\limits_j C_j z_j^2 \right)^{1/2}$

e = Elementary charge

N = Avogadro's constant

ε = Dielectric constant of surrounding solution

k = Boltzmann's constant

T = Absolute temperature

C_j = Equilibrium concentration of ion j

z_j = Valence of ion j, sign included

For aqueous solutions at 20°C, equation 4.1 becomes

$$S = B \times 10^9 \; V_t \frac{\Delta C_1}{C_1} \sqrt{C_1} \tag{4.2}$$

The values for the constants A' and B for various electrolyte types, in the presence of a negatively charged surface, are listed in Table 4.1 [5].

The van den Hul and Lyklema equation was developed for a constant potential surface. Schofield derived a similar equation for the condition of constant charge [6]. The equation is presented here

$$\frac{\Gamma}{C} = \frac{q}{\sqrt{C\beta_1}} - \frac{4}{\beta\Gamma} \tag{4.3}$$

where

Γ_- = Negative adsorption of repelled ions per unit area
(gram ions/cm^2)

q = Factor depending on the cationic:anionic valence ratio p [6]

$\beta = \dfrac{8\pi Ne^2}{\varepsilon RT}$

Γ = Surface density of charge (meq/cm^2)

Schofield's equation for the case of low charge density is equivalent to van den Hul and Lyklema's equation for the case of low potential. The two equations written for high charge or high potential situations are identical.

The equation to be used depends on whether the surface is one of constant charge or constant potential. The borosilicate gels used in this research are constant potential surfaces. Since a suitable bulk solution would be an aqueous NaCl mixture, the appropriate relationship is given by equation 4.2. The specific surface area was desired so that various samples could be compared. Therefore, both sides of equation 4.2 were divided by the mass of the sample. The modified equation, with the appropriate constant B, follows below.

$$S' = 5.2 \times 10^8 \; \frac{V_t \Delta C_1}{m\sqrt{C_1}} \tag{4.4}$$

where

S' = Surface area per unit mass (cm^2/g)

m = mass of sample (g)

Experimental Procedure

The negative adsorption procedure presented below was used to measure the specific surface areas of the gels described later.

Apparatus:

    (1) pH meter, Corning model 150

    (2) Chloride ion determining electrode, Corning 476126

    (3) Reference electrode, Corning double junction 476067

    (4) 300 ml polypropylene beakers, one for each gel sample

    (5) 100 ml polypropylene beakers, one for each measurement

    (6) Parafilm, used to seal 300 ml beakers

    (7) 100 ml graduated cylinder

    (8) 25 ml pipette

    (9) Pipette suction bulb

Materials:

    (1) Gel samples

    (2) 0.1 N NaCl solution, 100 ml for each gel sample

    (3) Various concentration of NaCl solutions for calibration of chloride electrode

    (4) 1.0 M KNO_3 buffer solution, 25 ml for each measurement

Preparation of Samples:

    (1) Weigh wet gel samples.

    (2) Place each sample in 300 ml beaker with 100 ml of 0.1 N NaCl solution.

    (3) Seal beakers with Parafilm.

    (4) Set aside for 3 weeks to equilibrate.

Procedure:

(1) Set up the pH meter according to instruction manual.

(2) Calibrate the chloride electrode as instructed in the manual.

(3) Once the gel samples have equilibrated, remove 25 ml of the bulk solution with a pipette.

(4) Place this solution in a 100 ml beaker.

(5) Add an equal volume of the 1.0 M KNO_3 buffer solution.

(6) Measure the absolute mV for the solution.

(7) Convert the data to concentration using the calibration information obtained earlier.

(8) Calculate the surface area per unit mass using Equation 4.4.

Al_2O_3 samples were used to develop the negative adsorption procedure. The surface areas of activated aluminum oxide and aluminum oxide gamma samples were determined using 1.0 N KCl, 0.1 N KCl, and 0.01 N KCl solutions with a 0.2 M KNO_3 buffer solution.

The basic steps in the procedure were not changed for the borosilicate gels. However, only one solution concentration was necessary and the solution chosen was 0.1 N NaCl since this was the same electrolyte used in the mechanistic experiment. Also, this particular concentration could be measured without dilution using a chloride ion determining electrode. The concentration of the buffer solution was increased when a newer instruction manual was found which recommended a 1.0 M KNO_3 solution for the chloride electrode used.

Two gel samples were provided for each of the following gel compositions: SiO_2, $SiO_2 \cdot \frac{1}{4}B_2O_3$, $SiO_2 \cdot \frac{1}{2}B_2O_3$, $SiO_2 \cdot \frac{3}{4}B_2O_3$, $SiO_2 \cdot B_2O_3$, $SiO_2 \cdot 1\frac{1}{2}B_2O_3$ and $SiO_2 \cdot 2B_2O_3$. Two 25 ml portions were drawn from the 100 ml of bulk

solution for each gel sample. Thus, four measurements were made for each
gel composition and the average of these results was reported. The 95%
confidence intervals were calculated using the pooled standard deviation
and a double sided t-distribution [7].

Experimental Results

Aluminum Oxide Results. The surface areas for the two Al_2O_3 samples
in the various solutions are presented in Table 4.2. Although it is
possible to calculate the surface area from the negative adsorption at only
one point, van den Hul and Lyklema suggested a procedure which involved
at least three different concentrations [5]. The data was plotted in the
form of $\frac{\Delta C_1}{m}$ vs. $\frac{\sqrt{C_1}}{V_t}$, and the surface area was calculated using the slope
of the line which most closely fits these points while going through the
origin. The Al_2O_3 plots are shown in Figure 4.1 and the resulting surface
areas are listed in Table 4.2. It was assumed that the surface area of
the sample was independent of the electrolyte concentration, even when the
higher concentrations were ten times the lower concentrations. The mech-
anistic experiment results presented in Chapter II demonstrated that the
borosilicate gel volumes were influenced by the electrolyte concentrations.
The aluminum oxide results in Table 4.2 show an increase in surface area
with increasing electrolyte concentration. Although this trend is the
opposite of that observed for borosilicate, it means that the surface areas
will not be constant. Therefore, using the slope over a range of elec-
trolyte concentrations to determine the surface area at one concentration
is invalid.

Borosilicate Gel Results. The surface areas for the borosilicate gels
are presented in Table 4.3 and in Figure 4.2. This plot shows that the
surface areas increased with increasing borate content of the gels. This

trend is consistent with the results of the 2^4 factorial design experiment and the mechanistic experiment. The effect of the electrolyte concentration on the surface area was not investigated since only one NaCl concentration was used. Several different NaCl concentrations could have been employed to obtain the values needed to determine the effect of the electrolyte concentration. However, the objective at this point was developing a technique rather than generating data.

One data point deviated from the observed trend. The $SiO_2 \cdot \frac{3}{4}B_2O_3$ surface area is more than three times that of the gels closest to it in composition. It is not known what caused such a discrepancy, but perhaps both samples were uncharacteristic of this particular gel composition. Another break in the data occurs with the two gels with the highest borate concentrations. These gel compositions were only used in the negative adsorption experiment, so their behavior has not been noted previously. It is possible that there is a change in swelling behavior between the $SiO_2 \cdot B_2O_3$ and the $SiO_2 \cdot 1\frac{1}{2}B_2O_3$ gels which results in larger volumes for the gels with the higher borate content. Water-to-solids mass ratios and specific volume data for these two gel compositions would help in understanding the situation.

Discussion

Teichner and co-workers have determined surface areas for inorganic oxide aerogels. They used the BET method on dry gels. However, the solvent in the gels was removed under hypercritical conditions in an autoclave. The resulting aerogels are believed to retain the original texture of the wet gels unlike gels dried at ambient pressures. Thus, it is reasonable to use Teichner and co-workers' surface area measurements for a comparison with the negative adsorption results of this study. They

found specific surface areas for silica aerogels on the order of 1×10^7 cm^2/g. Most of the negative adsorption values for the borosilicate gels are within 40% of this number. Therefore, this procedure produces reasonable specific surface areas.

Sources of errors in this negative adsorption procedure include the volume measurements, the wet gel weight, the chloride electrode calibration and the chloride ion measurements. The volumes of the total solution, the solution drawn from the bulk solution and the buffer solution are important. The total volume is included in the calculation of the surface area and the calibration of the chloride electrode is based on equal volumes of solution and buffer. Also, the solution must be drawn from the bulk solution, as far as possible from the gel sample. As with the mechanistic experiment, the mass of the wet gel is influenced by the amount of water on the surface of the gel that is blotted before weighing. The careful calibration of the chloride electrode is most important, since the change associated with the negative adsorption may only be 0.1 mV. Any errors in these measurements are amplified, since the relationship between the mV reading and the chloride concentration involves the log of the concentration. In addition, the calibration should be conducted at the same time as the surface area measurements because the long-term drift of the chloride electrode is in the range of 1 to 2 mV per day. The calculated error bars, at a 95% confidence interval, are about half the magnitude of most of the specific surface areas. Increasing the size and the number of samples for each gel composition would reduce the size of the error bars.

In the future the negative adsorption measurement can be incorporated with the mechanistic experimental procedure. After the four week soaking

period, a portion of the NaCl solution could be drawn off. With the higher electrolyte concentrations, this solution would have to be diluted since the highest concentration the chloride electrode can measure accurately is 10^{-1} N. The concentration of the solution would then be determined and the surface area calculated. The gel sample could be used for water-to-solids mass ratio or specific volume measurements as well.

Conclusions

A negative adsorption procedure was developed to measure the specific surface areas of the borosilicate gels since a change in surface area is another indication of the degree of swelling or syneresis. This method was more appropriate than dry techniques because the gels remain in a NaCl solution similar to those used in the mechanistic experiment. Specific surface areas were measured for SiO_2, $SiO_2 \cdot \frac{1}{4} B_2 O_3$, $SiO_2 \cdot \frac{1}{2} B_2 O_3$, $SiO_2 \cdot \frac{3}{4} B_2 O_3$, $SiO_2 \cdot B_2 O_3$, $SiO_2 \cdot 1 \frac{1}{2} B_2 O_3$ and $SiO_2 \cdot 2 B_2 O_3$ and ranged from 1.59×10^6 to 2.05×10^7 cm^2/g. These surface areas are similar in magnitude to published values for silica aerogels determined using BET procedures. The values tended to increase with increasing borate content of the gels which is consistent with the results of the mechanistic experiment.

References

[1] Mackenzie, J. D. "Applications of Sol—Gel Methods for Glass and Ceramics Processing" in *Ultrastructure Processing of Ceramics, Glasses and Composites*, edited by Larry L. Hench and Donald R. Ulrich. New York: John Wiley and Sons, 1984.

[2] Zelinski, B. J. J. and D. R. Uhlmann. "Gel Technology in Ceramics," *Journal of Physical Chemistry and Solids*, 45: 1069–1090 (1984).

[3] Adamson, Arthur W. *Physical Chemistry of Surfaces*, 4th Edition. New York: John Wiley and Sons, 1982.

[4] James, Robert O. and George A. Parks. "Characterization of Aqueous Colloids by Their Electrical Double-Layer and Intrinsic Surface Chemical Properties" in *Surface and Colloid Science, Volume 12*, edited by Egon Matijevic. New York: John Wiley and Sons, 1980.

[5] van den Hul, H. J. and J. Lyklema. "Determination of Specific Surface Areas of Dispersed Materials by Negative Adsorption," *Journal of Colloid and Interface Science*, 23: 500–508 (1967).

[6] Schofield, R. Kenworthy. "Calculation of Surface Areas from Measurements of Negative Adsorption," *Nature*, 160: 408–410 (September 20, 1947).

[7] Course notes from "Strategy of Experimentation," DuPont Professional Training Seminars, copyright 1974.

[8] Teichner, S. J. and *et al*. "Inorganic Oxide Aerogels," *Advances in Colloid and Interface Science*, 5: 245–273 (1976).

Table 4.1. Constants A' and B of Equations 4.1 and 4.2 for Various Electrolyte Types in the Presence of a Negatively Charged Surface [5].

z_+	z_-	A'	B*
z	z	2.0	0.52z
2	1	1.268	1.42
3	1	0.943	2.69
1	2	3.0	0.60
1	3	3.743	0.68

* for C_1 [=] $moles/cm^3$

Table 4.2. Measured Specific Surface Areas for Two Al_2O_3 Samples

Sample	Solution Concentration (N)	Surface Area from Single Point (cm^2/g)	Surface Area from Slope (cm^2/g)
Al_2O_3	1.0 N KCl	$9.01 \times 10^6 \pm 1.6 \times 10^6$	–
activated	0.1 N KCl	$3.75 \times 10^6 \pm 1.6 \times 10^6$	–
	0.01 N KCl	$1.84 \times 10^6 \pm 1.6 \times 10^6$	–
	–	–	8.50×10^6
Al_2O_3	1.0 N KCl	$1.26 \times 10^7 \pm 2.0 \times 10^6$	–
gamma	0.1 N KCl	$5.98 \times 10^6 \pm 2.0 \times 10^6$	–
	0.01 N KCl	$1.39 \times 10^6 \pm 2.0 \times 10^6$	–
	–	–	1.20×10^7

Table 4.3. Measured Specific Surface
Areas for Various Borosilicate Gels

Gel Type	Surface Area (cm^2/g)
SiO_2	$6.02 \times 10^6 \pm 3.8 \times 10^6$
$SiO_2 \cdot \frac{1}{4} B_2 O_3$	$2.45 \times 10^6 \pm 3.8 \times 10^6$
$SiO_2 \cdot \frac{1}{2} B_2 O_3$	$4.40 \times 10^6 \pm 3.8 \times 10^6$
$SiO_2 \cdot \frac{3}{4} B_2 O_3$	$2.05 \times 10^7 \pm 3.8 \times 10^6$
$SiO_2 \cdot B_2 O_3$	$1.59 \times 10^6 \pm 3.8 \times 10^6$
$SiO_2 \cdot 1\frac{1}{2} B_2 O_3$	$1.35 \times 10^7 \pm 3.8 \times 10^6$
$SiO_2 \cdot 2 B_2 O_3$	$1.13 \times 10^7 \pm 3.8 \times 10^6$
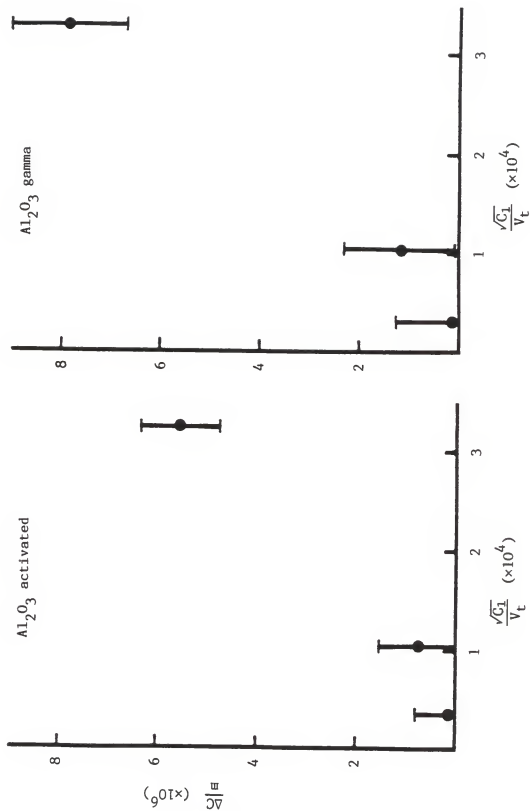
Figure 4.1. Negative Adsorption Plots for Two Al_2O_3 Samples.
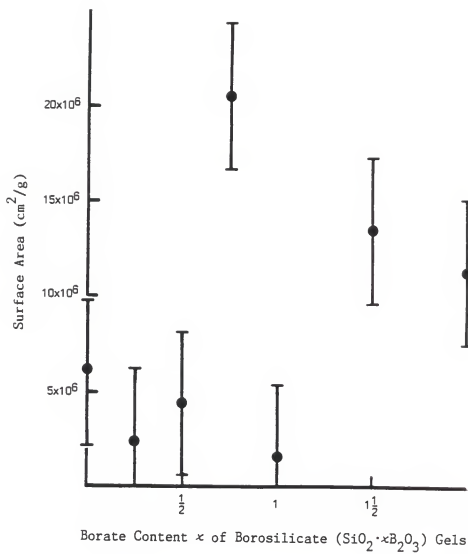
Figure 4.2. Surface Areas for Various Borosilicate Gels.

V. Conclusions

The major disadvantage of the sol-gel techniques used in preparing monolithic ceramic materials is the large, uncontrolled shrinkage of the gel during the drying process. The goal of this research has been to reduce the magnitude of this problem by first minimizing the gel volumes in the wet state. This was accomplished by placing the gels in solutions which induced syneresis. In doing so, the effects resulting from the gelation process were isolated from the effects due to the syneresis phenomena in the post-gelation step.

Important variables in the syneresis of borosilicate gels were identified using a 2^4 factorial design experiment. The solvent content of the gels decreased with decreasing valence, increasing electrolyte concentration, increased rinsing and decreasing borate concentration. The effect of pH was not statistically significant.

The information provided by the design experiment was used to develop a more detailed, mechanistic experiment. Swelling data of borosilicate gels were obtained as a function of borate content of the gel and electrolyte concentration of the solvent. The water-to-solids mass ratios decreased with increasing NaCl concentration and decreasing borate content. The effect appeared to be linear for low borate concentrations and non-linear for higher borate concentrations. The solvent content decreased by about 20% at the lower borate concentrations and by as much as 40% at the higher borate concentrations. The trend remained after a preliminary correction for the salt content of the solution, although the changes were only about a third as large. Specific volume measurements were consistent with the previous results.

Changes in the surface areas are another measure of the degree of

swelling or syneresis. Therefore, a negative adsorption procedure has been presented which is capable of determining specific surface areas of borosilicate gels in equilibrium with electrolyte. This procedure could be used to measure specific surface areas of gels while studying their swelling behavior in solutions with different concentrations. The surface area measurements of borosilicate gels in NaCl solutions made with this technique decreased with decreasing borate content of the gels. The effect was non-linear indicating a possible change in swelling behavior which resulted in larger volumes for the gels with the higher borate content.

Appendix <u>A</u>

The Minimum Significant Factor Effect and Minimum
Curvature Calculations for SiO_2 and $SiO_2 \cdot B_2O_3$

Table A.1. Calculations for SiO_2 Results.

Trial	Mass Water Mass Solids		Average Value	Degrees of Freedom	Standard Deviation	
	y		$\bar{y}$	$(n_i - 1)$	s	$(n_i - 1)s^2$
1	1.441	1.492	1.467	1	0.0361	0.0013
2	1.300	1.393	1.346	1	0.0658	0.0043
3	1.229	1.000	1.114	1	0.1619	0.0262
4	1.550	1.476	1.513	1	0.0523	0.0027
5	1.736	1.517	1.627	1	0.1549	0.0240
6	1.633	1.929	1.781	1	0.2093	0.0438
7	1.187	1.097	1.142	1	0.0636	0.0041
8	1.329	1.447	1.388	1	0.0834	0.0070
9	1.896	1.158	1.527	1	0.5218	0.2723
10	1.611	1.604	1.608	1	0.0050	0.0000
11	1.430	1.245	1.337	1	0.1308	0.0171
12	1.566	1.707	1.636	1	0.0997	0.0099
13	1.720	1.481	1.601	1	0.1690	0.0286
14	1.425	1.550	1.488	1	0.0884	0.0078
15	1.513	1.344	1.429	1	0.1195	0.0143
16	1.771	1.593	1.682	1	0.1259	0.0158
17	1.374	1.356	1.386	3	0.0996	0.0298
	1.525	1.289				
				$\Sigma = 19$		$\Sigma = 0.5090$

$$s_{pooled}^2 = \frac{\Sigma(n_i - 1)s^2}{\Sigma(n_i - 1)} = 0.0268 \qquad s_{pooled} = 0.1637$$

At a confidence interval of 90%:

$$[min] = ts\sqrt{2/mk} = 1.73(0.1637)\sqrt{2/(8)(2)} = 0.100$$
$$[min\ C] = ts\sqrt{1/mk + 1/C} = 1.73(0.1637)\sqrt{1/(16)(2) + 1/4} = 0.150$$

Table A.2. Calculations for $SiO_2 \cdot B_2O_3$ Results.

Trial	Mass Water Mass Solids y		Average Value $\bar{y}$	Degrees of Freedom $(n_i - 1)$	Standard Deviation s	$(n_i - 1)s^2$
1	2.451	3.449	2.950	1	0.7057	0.4980
2	2.315	3.536	2.926	1	0.8634	0.7454
3	1.781	2.646	2.214	1	0.6116	0.3741
4	2.248	2.905	2.577	1	0.4646	0.2158
5	2.287	2.187	2.237	1	0.0707	0.0050
6	2.357	2.594	2.475	1	0.1676	0.0281
7	1.659	1.958	1.809	1	0.2114	0.0447
8	2.233	2.609	2.421	1	0.2659	0.0707
9	2.533	3.854	3.194	1	0.9341	0.8725
10	2.603	3.956	3.280	1	0.9567	0.9153
11	3.049	2.930	2.990	1	0.0841	0.0071
12	2.442	3.889	3.166	1	1.0232	1.0459
13	3.204	3.643	3.424	1	0.3104	0.0964
14	2.997	3.520	3.259	1	0.3698	0.1368
15	2.367	2.313	2.340	1	0.0382	0.0015
16	2.625	4.367	3.496	1	1.2318	1.5173
17	3.458	2.854	2.896	3	0.3918	0.4604
	2.576	2.695				
				$\Sigma = 19$		$\Sigma = 7.0350$

$$s_{pooled}^2 = \frac{\Sigma(n_i - 1)s^2}{\Sigma(n_i - 1)} = 0.3703 \qquad s_{pooled} = 0.6085$$

At a confidence interval of 90%:

$[min] = ts\sqrt{2/mk} = 1.73(0.6085)\sqrt{2/(8)(2)} = 0.372$

$[min\ C] = ts\sqrt{1/mk + 1/C} = 1.73(0.6085)\sqrt{1/(16)(2) + 1/4} = 0.558$

Appendix B

Adjusted SiO_2 and $SiO_2 \cdot B_2O_3$ Values and Their
Graphical and Computational Analyses

Table B.1. Calculations for SiO_2 Adjusted Results.

Trial	y Adjusted		Average Value $\bar{y}$	Degrees of Freedom $(n_i - 1)$	Standard Deviation s	$(n_i - 1)s^2$
1	0.064	0.031	0.048	1	0.0234	0.0006
2	0.156	0.095	0.126	1	0.0427	0.0018
3	0.202	0.351	0.276	1	0.1052	0.0111
4	−0.006	0.042	0.018	1	0.0340	0.0012
5	−0.127	0.015	−0.056	1	0.1006	0.0101
6	−0.060	−0.253	−0.156	1	0.1359	0.0185
7	0.229	0.228	0.258	1	0.0413	0.0017
8	0.137	0.060	0.099	1	0.0542	0.0029
9	−0.231	0.248	0.008	1	0.3389	0.1148
10	−0.046	−0.042	−0.044	1	0.0032	0.0000
11	0.071	0.192	0.131	1	0.0849	0.0072
12	−0.017	−0.108	−0.063	1	0.0647	0.0042
13	−0.117	0.039	−0.039	1	0.1099	0.0121
14	0.075	−0.006	0.034	1	0.0574	0.0033
15	0.018	0.127	0.072	1	0.0776	0.0060
16	−0.150	−0.034	−0.092	1	0.0817	0.0067
17	0.108	0.119	0.100	3	0.0647	0.0126
	0.010	0.163		$\Sigma = 19$		$\Sigma = 0.2148$

$$y_{blank} = 1.540 \frac{\text{Mass Water}}{\text{Mass Solids}} \qquad y_{adjusted} = \frac{y_{blank} - y_{observed}}{y_{blank}}$$

$$s_{pooled}^2 = \frac{\Sigma(n_i - 1)s^2}{\Sigma(n_i - 1)} = 0.0113 \qquad s_{pooled} = 0.1063$$

At a confidence interval of 90%

$$[\text{min}] = ts\sqrt{2/mk} = 1.73(0.1063)\sqrt{2/(8)(2)} = 0.065$$
$$[\text{min C}] = ts\sqrt{1/mk + 1/C} = 1.73(0.1063)\sqrt{1/(16)(2) + 1/4} = 0.098$$

Table B.2. Calculations for $SiO_2 \cdot B_2O_3$ Adjusted Results.

Trial	y Adjusted		Average Value $\overline{y}$	Degrees of Freedom $(n_i - 1)$	Standard Deviation s	$(n_i - 1)s^2$
1	-0.576	-1.218	-0.897	1	0.4538	0.2060
2	-0.489	-1.274	-0.881	1	0.5552	0.3083
3	-0.145	-0.702	-0.423	1	0.3933	0.1547
4	-0.446	-0.868	-0.657	1	0.2988	0.0893
5	-0.471	-0.406	-0.439	1	0.0455	0.0021
6	-0.516	-0.668	-0.592	1	0.1078	0.0116
7	-0.067	-0.259	-0.163	1	0.1360	0.0185
8	-0.436	-0.678	-0.557	1	0.1710	0.0292
9	-0.629	-1.478	-1.054	1	0.6007	0.3608
10	-0.674	-1.544	-1.109	1	0.6153	0.3785
11	-0.961	-0.884	-0.923	1	0.0541	0.0029
12	-0.570	-1.501	-1.036	1	0.6580	0.4330
13	-1.060	-1.343	-1.202	1	0.1996	0.0399
14	-0.927	-1.264	-1.096	1	0.2378	0.0566
15	-0.522	-0.487	-0.505	1	0.0246	0.0006
16	-0.688	-1.808	-1.248	1	0.7921	0.6275
17	-1.223	-0.835	-0.855	3	0.2570	0.1981
	-0.657	-0.705		$\Sigma = 19$		$\Sigma = 2.9176$

$$y_{blank} = 1.555 \frac{\text{Mass Water}}{\text{Mass Solids}} \qquad y_{adjusted} = \frac{y_{blank} - y_{observed}}{y_{blank}}$$

$$s^2_{pooled} = \frac{\Sigma(n_i - 1)s^2}{\Sigma(n_i - 1)} = 0.1536 \qquad s_{pooled} = 0.3919$$

At a confidence interval of 90%:

$$[min] = ts\sqrt{2/mk} = 1.73(0.3919)\sqrt{2/(8)(2)} = 0.240$$
$$[min~C] = ts\sqrt{1/mk + 1/C} = 1.73(0.3919)\sqrt{1/(16)(2) + 1/4} = 0.360$$

Table B.3. Computational Analysis of SiO_2 Adjusted.

Trial	$\bar{y}$	Mean	x_1	x_2	x_3	x_4	x_1x_2	x_1x_3	x_1x_4	x_2x_3	x_2x_4	x_3x_4	$x_1x_2x_3$	$x_1x_2x_4$	$x_1x_3x_4$	$x_2x_3x_4$	$x_1x_2x_3x_4$
1	0.048	+	−	−	−	−	+	+	+	+	+	+	−	−	−	−	+
2	0.126	+	+	−	−	−	−	−	−	+	+	+	+	+	+	−	−
3	0.276	+	−	+	−	−	−	+	+	−	−	+	+	+	−	+	−
4	0.018	+	+	+	−	−	+	−	−	−	−	+	−	−	+	+	+
5	−0.056	+	−	−	+	−	+	−	+	−	+	−	+	−	+	+	−
6	−0.156	+	+	−	+	−	−	+	−	−	+	−	−	+	−	+	+
7	0.258	+	−	+	+	−	−	−	+	+	−	−	−	+	+	−	+
8	0.099	+	+	+	+	−	+	+	−	+	−	−	+	−	−	−	−
9	0.008	+	−	−	−	+	+	+	−	+	−	−	−	+	+	+	−
10	−0.044	+	+	−	−	+	−	−	+	+	−	−	+	−	−	+	+
11	0.131	+	−	+	−	+	−	+	−	−	+	−	+	−	+	−	+
12	−0.063	+	+	+	−	+	+	−	+	−	+	−	−	+	−	−	−
13	−0.039	+	−	−	+	+	+	−	−	−	−	+	+	+	−	−	+
14	0.034	+	+	−	+	+	−	+	+	−	−	+	−	−	+	−	−
15	0.072	+	−	+	+	+	−	−	−	+	+	+	−	−	−	+	−
16	−0.092	+	+	+	+	+	+	+	+	+	+	+	+	+	+	+	+
sum+ =		0.620	−0.078	0.699	0.120	0.007	−0.077	0.348	0.361	0.475	0.010	0.443	0.401	0.318	0.427	0.026	0.124
sum− =		0.000	0.698	−0.079	0.500	0.613	0.697	0.272	0.259	0.145	0.610	0.177	0.219	0.302	0.193	0.594	0.496
overall sum =		0.620	0.620	0.620	0.620	0.620	0.620	0.620	0.620	0.620	0.620	0.620	0.620	0.620	0.620	0.620	0.620
Difference =		0.620	−0.776	0.778	−0.380	−0.606	−0.774	0.076	0.102	0.330	−0.600	0.266	0.182	0.016	0.234	−0.568	−0.372
Effect =		0.039	−0.097	0.097	−0.048	−0.076	−0.097	0.010	0.013	0.041	−0.075	0.033	0.023	0.002	0.029	−0.071	−0.047
			*	*	*	*	*				*					*	

(Trial 17) Center Point Average = 0.100

Curvature = 0.039 − 0.100 = −0.061   [min] = 0.065   [min C] = 0.098

Table B.4. Computational Analysis of $SiO_2 \cdot B_2O_3$ Adjusted.

Trial	$\bar{y}$ Mean		x_1	x_2	x_3	x_4	x_1x_2	x_1x_3	x_1x_4	x_2x_3	x_2x_4	x_3x_4	$x_1x_2x_3$	$x_1x_2x_4$	$x_1x_3x_4$	$x_2x_3x_4$	$x_1x_2x_3x_4$
1	-0.897	+	-	-	-	-	+	+	+	+	+	+	-	-	-	-	+
2	-0.881	+	+	-	-	-	-	-	-	+	+	+	+	+	+	-	-
3	-0.423	+	-	+	-	-	-	+	+	-	-	+	+	+	-	+	-
4	-0.657	+	+	+	-	-	+	-	-	-	-	+	-	-	+	+	+
5	-0.439	+	-	-	+	-	+	-	+	-	+	-	+	-	+	+	-
6	-0.592	+	+	-	+	-	-	+	-	-	+	-	-	+	-	+	+
7	-0.163	+	-	+	+	-	-	-	+	+	-	-	-	+	+	-	+
8	-0.557	+	+	+	+	-	+	+	-	+	-	-	+	-	-	-	-
9	-1.054	+	-	-	-	+	+	+	-	+	-	-	-	+	+	+	-
10	-1.109	+	+	-	-	+	-	-	+	+	-	-	+	-	-	+	+
11	-0.923	+	-	+	-	+	-	+	-	-	+	-	+	-	+	-	+
12	-1.036	+	+	+	-	+	+	-	+	-	+	-	-	+	-	-	-
13	-1.202	+	-	-	+	+	+	-	-	-	-	+	+	+	-	-	+
14	-1.096	+	+	-	+	+	-	+	+	-	-	+	-	-	+	-	-
15	-0.505	+	-	+	+	+	-	-	-	+	+	+	-	-	-	+	-
16	-1.248	+	+	+	+	+	+	+	+	+	+	+	+	+	+	+	+
						*											
sum+ =	-12.782		-7.176	-5.512	-5.802	-8.173	-7.090	-6.790	-6.411	-6.414	-6.521	-6.909	-6.782	-6.599	-6.461	-6.027	-6.791
sum- =	0.000		-5.606	-7.270	-6.980	-4.609	-5.692	-5.992	-6.371	-6.368	-6.261	-5.873	-6.000	-6.183	-6.321	-6.755	-5.991
overall sum =	-12.782		-12.782	-12.782	-12.782	-12.782	-12.782	-12.782	-12.782	-12.782	-12.782	-12.782	-12.782	-12.782	-12.782	-12.782	-12.782
Difference =	-12.782		-1.570	1.758	1.178	-3.564	-1.398	-0.798	-0.040	-0.046	-0.260	-1.036	-0.782	-0.416	-0.140	-0.728	-0.800
Effect =	-0.799		-0.196	0.220	0.147	-0.446	-0.175	-0.100	-0.005	-0.006	-0.033	-0.130	-0.098	-0.052	-0.018	0.091	-0.100

(Trial 17) Center Point Average = -0.855

Curvature = -0.799 - (-0.855) = 0.056

[min] = 0.240   [min] = 0.240   [min C] = 0.360
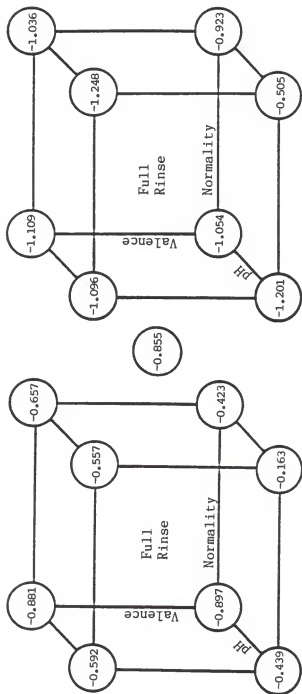
Figure B.1. Graphical Analysis for SiO_2 Adjusted Values
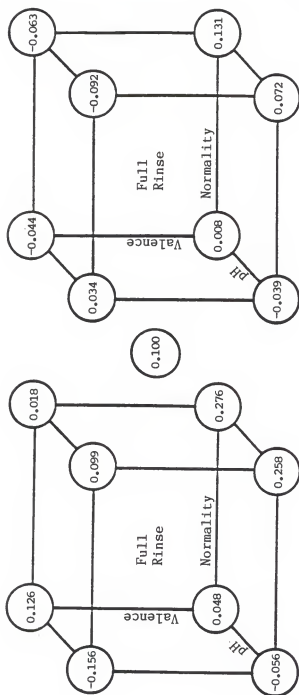
Figure B.2. Graphical Analysis for $SiO_2 \cdot B_2O_3$ Adjusted Values.

Appendix C

ASTM Procedure D 70: Standard Test Method for Specfic
Gravity and Density of Semi-solid Bituminous Materials

 Designation: D 70 – 82

Standard Test Method for
SPECIFIC GRAVITY AND DENSITY OF SEMI-SOLID
BITUMINOUS MATERIALS[1]

This standard is issued under the fixed designation D 70; the number immediately following the designation indicates the year of original adoption or, in the case of revision, the year of last revision. A number in parentheses indicates the year of last reapproval. A superscript epsilon (ε) indicates an editorial change since the last revision or reapproval.

1. Scope

1.1 This method covers the determinations of the specific gravity and density of semi-solid bituminous materials, asphalt cements, and soft tar pitches by use of a pycnometer.

2. Applicable Documents

2.1 *ASTM Standards:*

C 670 Practice for Preparing Precision Statements for Test Methods for Construction Materials[2]

D 140 Methods of Sampling Bituminous Materials[2]

E 1 Specification for ASTM Thermometers[3]

3. Significance and Use

3.1 Values of specific gravity and density are used for converting volumes to units of mass as required in other ASTM standards and in sales transactions.

4. Descriptions of Terms

4.1 *specific gravity*—*of some solid bituminous material, asphalt cement, and soft tar pitcher,* the ratio of the mass of a given volume of the material at 77°F (25°C) or at 60°F (15.6°C) to that of an equal volume of water at the same temperature, and is expressed as follows:

Specific Gravity, 77/77 F (25/25 C)

or 60/60 F (15.6/15.6 C)

4.2 *density*—the mass per unit of volume stated as follows:

Density, 77°F (25°C), g/cm³

or 60°F (15.6°C), g/cm³

5. Apparatus

5.1 *Pycnometer,* glass, consisting of a cylindrical or conical vessel carefully ground to

receive an accurately fitting glass stopper 22 to 26 mm in diameter. The stopper shall be provided with a hole 1.0 to 2.0 mm in diameter, centrally located in reference to the vertical axis. The top surface of the stopper shall be smooth and substantially plane, and the lower surface shall be concave in order to allow all air to escape through the bore. The height of the concave section shall be 4.0 to 6.0 mm at the center. The stoppered pycnometer shall have a capacity of 24 to 30 mL, and shall weigh not more than 40 g. Suitable pycnometers are illustrated in Fig. I.

5.2 *Water Bath,* constant-temperature, capable of maintaining the temperature within 0.2°F (0.1°C) of the test temperature.

5.3 *Thermometer,* calibrated liquid-in-glass, total immersion-type, of suitable range with graduations at least every 0.2°F (0.1°C) and a maximum scale error of 0.2°F (0.1°C) as prescribed in Specification E 1. Thermometers commonly used are 63F or 63C. Any other measurement device of equal accuracy may be used.

6. Bulk Sampling

6.1 Samples from shipments shall be taken in accordance with Methods D 140, and shall be free of foreign substances. Thoroughly mix

---

D 70

the sample before removing a representative portion for the determination.

7. Materials

7.1 *Distilled or Demineralized Water*—Freshly boiled and cooled distilled or deionized water shall be used to fill the pycnometer and the beaker.

8. Preparation of Equipment

8.1 Partially fill a 600-mL Griffin low-form beaker with freshly boiled and cooled distilled or deionized water to a level that will allow the top of the pycnometer to be immersed to a depth of not less than 40 mm.

8.2 Partially immerse the beaker in the water bath to a depth sufficient to allow the bottom of the beaker to be immersed to a depth of not less than 100 mm, while the top of the beaker is above the water level of the bath. Clamp the beaker in place.

8.3 Maintain the temperature of the water bath within 0.2°F (0.1°C) of the test temperature.

9. Calibration of Pycnometer

9.1 Thoroughly clean, dry, and weigh the pycnometer to the nearest 1 mg. Designate this weight as A.

9.2 Place the beaker from the water bath. Fill the pycnometer with freshly boiled distilled or deionized water, placing the stopper loosely in the pycnometer. Place the pycnometer in the beaker and press the stopper firmly in place. Return the beaker to the water bath.

NOTE 1—Calibration should be done at the specified temperature. A pycnometer calibrated at one temperature cannot be used at a different temperature without recalibration at that temperature.

9.3 Allow the pycnometer to remain in the water for a period of not less than 30 min. Remove the pycnometer, immediately dry the top of the stopper with one stroke of a dry towel (Note 2), then quickly dry the remaining outside of the pycnometer and weigh to the nearest 1 mg. Designate the weight of the pycnometer plus water as B.

NOTE 2—Do not rub the top of the stopper even if a small amount of water or an air expansion, if the cap is dried at the instant of removing the pycnometer from the water, the proper weight of the pycnometer plus water can be recorded. If moisture condenses on the pycnometer during weighing, wipe the outside of the pycnometer (excluding the top) before recording the weight.

10. Procedure

10.1 *Preparation of Sample*—Heat the sample with care, stirring to prevent local overheating, until the sample has become sufficiently fluid to pour. In no case should the temperature be raised to more than 100°F (56°C) above the expected softening point for tar, or to more than 200°F (111°C) above the expected softening point for asphalt. Do not heat for more than 30 min, and avoid incorporating air bubbles into the clean, dry, warmed pycnometer to fill it about three fourths of its capacity. Take precautions to keep the material from touching the sides of the pycnometer above the final level, and to prevent the inclusion of air bubbles (Note 3). Allow the pycnometer and its contents to cool to ambient temperature for a period of not less than 40 min, and weigh with the stopper to the nearest 1 mg. Designate the weight of the pycnometer plus sample as C.

NOTE 3—If any air bubbles are inadvertently included, remove by brushing the surface of the asphalt with flame from a small gas or alcohol burner. In order to avoid overheating, do not allow the flame to remain in contact with the sample more than a few seconds at any one time.

10.3 Remove the beaker from the water bath. Fill the pycnometer containing the asphalt with freshly boiled distilled or deionized water, placing the stopper loosely in the pycnometer. Do not allow any air bubbles to remain in the pycnometer. Place the pycnometer in the beaker and press the stopper firmly in place. Return the beaker to the water bath.

10.4 Allow the pycnometer to remain in the water bath for a period of not less than 30 min. Remove the pycnometer from the bath. Dry and weigh using the same technique and timing as that employed in 9.3. Designate this weight of pycnometer plus sample plus water as D.

11. Calculations

11.1 Calculate the specific gravity to the nearest 0.001 as follows:

Specific gravity $= (C - A)/[(B - A) - (D - C)]$

where:

A = weight of pycnometer (glass stopper),

B = weight of pycnometer filled with water,

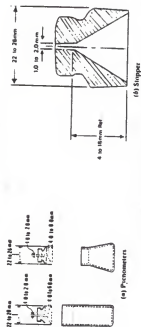C = weight of pycnometer partially filled with asphalt, and

FIG. 1 Suitable Pycnometers and Stopper

D = weight of pycnometer plus asphalt plus water.

11.2 Calculate density to the nearest 0.001 as follows:

$$\text{Density} = \text{specific gravity} \times W_T$$

where:

specific gravity = calculation from 11.1, and
W_T = density of water at test temperature in desired units (Note 4).

NOTE 4—Density of water from Handbook of Chemistry Physics, 45th Ed.

Test Temperature, °F (°C)	Density of Water, lb/gal (g/cm³)
60 (15.6)	8.337 (0.9990)
77 (25)	8.321 (0.9971)

12. Report

12.1 Report specific gravity and density to the nearest third decimal and the test temperature of 77/77°F (25/25°C) or 60/60°F (15.6/15.6°C).

13. Precision

13.1 Single-Operator Precision—The single-operator standard deviation for specific gravity of semi-solid bituminous materials tested at 60°F (15.6°C) has been found to be 0.0013 (Note 5). Therefore, results of two properly conducted tests by the same operator on the same material should not differ by more than 0.003 (Note 5).

13.1.1 For materials tested at 77°F (25°C),

the standard deviation has been found to be 0.00082 (Note 5). Therefore, results of two properly conducted tests by the same operator should not differ by more than 0.002 (Note 5).

13.1.2 Results of properly conducted tests for density by the same operator should not differ by more than the following values:

Test Temperature, °F (°C)	Density, lb/gal (g/cm³)
60 (15.6)	0.020 (0.002)
77 (25)	0.017 (0.002)

13.2 Multilaboratory Precision—The multilaboratory standard deviation for semi-solid bituminous materials tested at 60°F (15.6°C) has been found to be 0.0024 (Note 5). Therefore, results of two properly conducted tests from two different laboratories on samples of the same material should not differ by more than 0.007 (Note 5).

13.2.1 For material tested at 77°F (25°C), the standard deviation has been found to be 0.0019 (Note 5). Therefore, results of two properly conducted tests from two different laboratories on samples of the same material should not differ by more than 0.005 (Note 5).

13.2.2 Results of two properly conducted tests from two different laboratories for density on samples of the same material should not differ by more than these values:

Test Temperature, °F (°C)	Density, lb/gal (g/cm³)
60 (15.6)	0.058 (0.007)
77 (25)	0.041 (0.005)

NOTE 5—These numbers represent, respectively, the (1S) and (D2S) limits as described in Practice C670.

TABLE 1 Precision of Specific Gravity Data for Semi-Solid Bituminous Materials

	Temperature °F (°C)	Single-Operator			Multilaboratory		
		Degrees of Freedom	(1S)	(D2S)	Degrees of Freedom	(1S)	(D2S)
Asphalt	60 (15.6)	54	0.0011	0.0032	24	0.0018	0.0051
	77 (25.0)	54	0.00080	0.0023	24	0.0024	0.0068
Soft tar pitch	60 (15.6)	72	0.0013	0.0038	27	0.0029	0.0083
	77 (25.0)	72	0.00083	0.0023	27	0.0017	0.0048
Pooled values	60 (15.6)	114	0.0013	0.0035	51	0.0024	0.0067
	77 (25.0)	114	0.00082	0.0023	51	0.0019	0.0053

THE CONTROL OF SWELLING AND SYNERESIS

IN BOROSILICATE GELS USING

COLLOIDAL PHENOMENA

by

BARBARA LINDHOLM ANGELL

B.S., Kansas State University, 1983

AN ABSTRACT OF A MASTER'S THESIS

submitted in partial fulfillment of the

requirements for the degree

MASTER OF SCIENCE

College of Engineering
Department of Chemical Engineering

KANSAS STATE UNIVERSITY
Manhattan, Kansas

1986

Abstract

The goal of this research was to reduce the shrinkage problems associated with the drying procedure in the sol-gel methods by first minimizing the gel volumes in the wet state. The approach used was to place the gels in solutions to induce swelling or syneresis. In doing so, the effects resulting from the gelation process were isolated from the effects due to the syneresis phenomena in the post-gelation step.

A 2^4 factorial design experiment was conducted to identify important solvent and gel preparation variables based upon their effects on the solvent content of borosilicate gels. The solvent variables (and the values studied) were electrolyte valence (Na^+ to Al^{3+}), electrolyte concentration (0.0 N to 1.0 N) and pH (4 to 10). The gel preparation variables included composition (SiO_2 to $SiO_2 \cdot B_2O_3$) and rinsed state (no rinse to full rinse). The water-to-solids mass ratios of the wet gels decreased with decreasing valence, increasing electrolyte concentration, increased rinsing and decreasing borate concentration. The effect of pH was not statistically significant.

A mechanistic experiment was planned using information obtained from the design experiment. This experiment included rinsed gels of five compositions (SiO_2, $SiO_2 \cdot \frac{1}{4}B_2O_3$, $SiO_2 \cdot \frac{1}{2}B_2O_3$, $SiO_2 \cdot \frac{3}{4}B_2O_3$ and $SiO_2 \cdot B_2O_3$) and eleven NaCl solutions (ranging from 0.0 N to 2.0 N), all at a pH of 4. The water-to-solids mass ratios and the specific volumes decreased with increasing NaCl concentration and decreasing borate concentration. The trends remained after correcting for the salt content of the solution. These volume changes were discussed in terms of the osmotic pressure and Donnal equilibrium.

A procedure based upon negative adsorption concepts was developed for

measuring the specific surface areas of the gels. Changes in the surface areas are another measure of the degree of swelling or syneresis. Initial results showed that the surface areas decreased with decreasing borate content for borosilicate gels in equilibrium with a 0.1 N NaCl solution.